

THE UNIVERSITY OF MICHIGAN
INDUSTRY PROGRAM OF THE COLLEGE OF ENGINEERING

THE DEVELOPMENT OF DISTURBANCES
IN SUPERCRITICAL FLOWS

James M. Wiggert

A dissertation submitted in partial fulfillment
of the requirements for the degree of
Doctor of Philosophy in the
University of Michigan
Department of Civil Engineering
1962

April, 1962

IP-558

Doctoral Committee:

Professor Ernest F. Brater, Co-Chairman
Professor Victor L. Streeter, Co-Chairman
Assistant Professor Walter R. Debler
Professor Maxwell O. Reade
Professor Chia-Shun Yih

PREFACE

To the co-chairmen of the committee goes the writer's gratitude for their ever ready counsel, guidance and support. To the committee members, for their valued criticism and patience, the writer expresses his thanks.

The University of Michigan and the Ford Foundation both contributed financial support. In addition, the Computing Center of the University was made available. All this support is gratefully acknowledged.

In recognizing the extent of the contribution of his family, who shared the burden without complaint, the writer finds that words are inadequate.

TABLE OF CONTENTS

	<u>Page</u>
PREFACE.....	ii
LIST OF FIGURES.....	iv
I. INTRODUCTION.....	1
II. HISTORY OF INSTABILITY INVESTIGATIONS.....	2
III. PHYSICAL EXPERIMENTS.....	8
IV. BASIS FOR COMPUTER METHOD.....	13
The Equations of Flow.....	13
The Method of Characteristics.....	17
The Formulation for the Computer Solution.....	23
The Convergence of the Solution.....	29
V. RESULTS OF COMPUTER COMPUTATION.....	32
VI. CONCLUSIONS.....	39
BIBLIOGRAPHY.....	59
APPENDIX.....	61

LIST OF FIGURES

<u>Figure</u>		<u>Page</u>
1	Plot of Depth Reynolds Number Versus Length Reynolds Number for the Occurrence of Roll Waves.....	11
2	Definition Sketch for Open Channel Flow.....	13
3	The Characteristic Curves and the Domain of Dependence.....	21
4	The Range of Influence.....	22
5	The Range of Influence of a Set of Initial Values.....	23
6	The Intersection of Characteristic Curves and Initial Data.....	25
7-14	Plots of the Computer Solutions of Non-Dimensional Depth and Velocity Versus Channel Length for Various Flow Parameters.....	41-58

I. INTRODUCTION

Roll waves are phenomena associated with steep channels, high velocities and small depths. Early observations were made by Cornish⁽²⁰⁾ of roll waves in drainage channels in the Alps. Photographs taken by Cornish remain one of the best illustrative examples of a periodic train of waves.

Roll waves are the result of the introduction of disturbances into an unstable uniform flow. These disturbances grow until they eventually break on the downstream side, forming small amplitude bores. Then the bores coalesce, the larger overtaking and incorporating the smaller, until a series of relatively large, periodic bores is the result. Bores of this type have come to be known as roll waves. A roll wave configuration is characterized by a wave speed greater than the uniform flow velocity in the downstream direction. The velocity in the cross section of the wave is considerably higher than the velocity in the section of shallower water.

Nearly all studies of the instability of flow in open channels start with consideration of a uniform flow, into which a disturbance is introduced. The disturbance is said to be a result of a slight protuberance in the channel itself, or some other factor affecting the uniform flow. This study pertains to the development with time of a disturbance introduced into an idealized uniform flow. The effects of changing the parameters describing the uniform flow are examined, as are the effects of the varying of parameters describing the disturbances.

II. HISTORY OF INSTABILITY INVESTIGATIONS

The stability of uniform flow can be examined by the introduction of a perturbation to the uniform flow. Consideration of existing formulas for hydraulic losses leads to the conclusion that the losses can be represented generally by the form

$$h_f = \kappa \frac{u^m}{R^n}$$

where u is the velocity and R the hydraulic radius. If consideration is limited to a wide open channel, the hydraulic radius is approximated by the depth, and the dynamic equation becomes (Figure 3)

$$-\frac{p_x}{\rho} + g \sin\theta - \kappa \frac{u^m}{h^n} = uu_x + u_t .$$

Introducing a hydrostatic assumption,

$$p_x = \gamma \cos\theta h_x ,$$

the dynamic equation can be written as

$$-g \cos\theta h_x + g \sin\theta - \kappa \frac{u^m}{h^n} = uu_x + u_t .$$

The continuity equation is

$$hu_x + uh_x + h_t = 0 .$$

If disturbances

$$u' = u'(x,t), \quad h' = h'(x,t)$$

are introduced to the uniform flow, then

$$u = u' + U, \quad h = h' + Y$$

where U and Y are uniform flow velocity and depth respectively.

Substitution of the perturbed flow variables into the dynamic and continuity equations gives

$$-g \cos\theta h'_x + g \sin\theta - \kappa \frac{(u'+U)^m}{(h'+Y)^n} = (u'+U)u'_x + u'_t ,$$

$$(h'+Y)u'_x + (u'+U)h'_x + h'_t = 0 .$$

Linearizing by dropping products of perturbations and their derivatives, and then subtracting the equation of uniform flow, the equations become

$$-g \cos\theta Y^n h'_x + g \sin\theta nY^{n-1}h' - \kappa mU^{m-1}u' = Y^n U u'_x + Y^n u'_t ,$$

$$Y u'_x + U h'_x + h'_t = 0 .$$

Assuming a potential exists for the perturbation velocities of the form

$$\phi = f(h)\exp(\alpha t + i\beta x);$$

then

$$u' = -\frac{\partial\phi}{\partial x} = -i\beta f(h)\exp(\alpha t + i\beta x),$$

$$u'_x = \beta^2 f(h)\exp(\alpha t + i\beta x),$$

$$u'_t = -i\gamma\beta f(h)\exp(\alpha t + i\beta x).$$

If the depth perturbation is of similar form

$$h' = f_2(h)\exp(\alpha t + i\beta x),$$

then

$$h'_x = i\beta f_2(h)\exp(\alpha t + i\beta x),$$

$$h'_t = \gamma f_2(h)\exp(\alpha t + i\beta x).$$

If the vertical perturbation velocity v' is introduced,

$$v' = -\frac{\partial\phi}{\partial h} = -f'(h)\exp(\alpha t + i\beta x).$$

But

$$v' = \frac{Dh'}{Dt} = h'_t + Uh'_x = (\alpha + i\beta U)f_2(h)\exp(\alpha t + i\beta x).$$

Equating expressions of v' ,

$$f_2(h) = - \frac{f'(h)}{(\alpha + i\beta U)} .$$

Then, substitution of the values of $f_2(h)$ into the expression for the depth perturbation and its derivatives, and substitution of the values of the depth and velocity perturbations and their derivatives into the continuity equation gives

$$f'(h) = \beta^2 Y f(h).$$

The same substitutions, along with the above value of $f'(h)$, when made into the dynamic equations, result in

$$\frac{g \cos\theta \ i\beta^2 Y}{\alpha + i\beta U} - \frac{g \sin\theta \ n\beta Y^n}{\alpha + i\beta U} + \kappa m i U^{m-1} = Y^n U \beta^2 - Y^n i \alpha .$$

Simplifying, and making the uniform flow substitution

$$Y^n g \sin\theta = \kappa U^m ,$$

the dynamic equation is written,

$$\alpha^2 + (2i\beta U + \frac{mg \sin\theta}{U})\alpha - \beta^2 U^2 + g \cos\theta \ Y\beta^2 + i(m+n)\beta g \sin\theta = 0.$$

Solving for α ,

$$\alpha = -i\beta U - \frac{mg \sin\theta}{2U} \pm \frac{1}{2} \left[\frac{m^2 g^2 \sin^2\theta}{U^2} - 4g \cos\theta \ Y\beta^2 - 4in\beta g \sin\theta \right]^{1/2} .$$

Requiring the real part of α to be equal to zero for the neutral case gives

$$\frac{U^2}{gY} = \frac{m^2}{n^2} \sqrt{\cos\theta} .$$

Introducing the Froude number

$$F = \frac{U}{\sqrt{gY}}$$

the stability criterion is written

$$F \begin{matrix} < \\ = \\ > \end{matrix} \frac{m}{n} \sqrt{\cos\theta} . \quad (1)$$

The flow is stable for the top two signs, unstable for the bottom sign.

The method of analysis employed above is essentially that of Jeffreys⁽¹⁾ and Dressler,⁽⁴⁾ and was performed by the writer before knowledge of Dressler's paper. While Jeffreys considered the case of Chezy resistance, the above treatment and that of Dressler permit use of general exponents in the resistance function. Dressler left the instability criterion in the form

$$m^{2n} g^2 - n^2 Y^{2m-n} \sin^2\theta \cong n^{2n} \kappa^2 \cos^n\theta .$$

Introduction of the uniform flow relationship to Dressler's criterion results in Equation (1). Substitution of a Chezy resistance form ($m=2, n=1$) into Equation (1) gives the familiar criterion for instability $F > 2$, since $\sqrt{\cos\theta} \cong 1$.

Thomas⁽²⁾ applied the concept of translating axis in order to obtain a steady flow configuration. This resulted in an equation of gradually varied flow. By categorizing profiles obtainable from his equation, Thomas found that only two of the possible profiles met necessary conditions at critical depth. From this he found the criterion of instability to be

$$\theta = \frac{1}{2} \sin^{-1} \frac{8g}{C^2}$$

where C^2 is the Chezy resistance coefficient ($U^2 = C^2RS$). For wide channels for which the angle of inclination θ , of the bottom is small,

$$\sin 2\theta \cong 2\theta,$$

$$S \cong \theta,$$

$$R \cong Y,$$

and the criterion reduces again to $F = 2$.

Vedernikov⁽⁵⁾ combined the dynamical and continuity equations, and considered the propagation velocity of the wavefront and the trajectory of a translation wave. From this he determined the variation of the propagation velocity of a given depth of the free surface. Considering the case when the variation of velocity of a given depth would represent an instability, he arrived at the criterion

$$\frac{(1-R \frac{dP}{dA})nU_0}{(W_0-U_0)^m} > 1,$$

where

$R =$ hydraulic radius.

$P =$ wetted perimeter.

$A =$ cross-sectional area.

$\left. \begin{matrix} n \\ m \end{matrix} \right\} =$ exponents in the law of resistance, $V^m = KSR^n$,
where S is the slope.

$W_0 =$ propagation velocity of the wave part in uniform flow.

$U_0 =$ uniform flow velocity.

For a wide, open-channel,

$$\frac{dP}{dA} \cong 0, \quad W = U + \sqrt{gh}$$

and for Chezy resistance

$$m = 2, \quad n = 1.$$

So Vedernikov's criterion becomes $F > 2$.

Schönfeld,⁽⁶⁾ using the concept of the characteristic directions of the wave components, found as the criterion of neutral stability,

$$U_0 = \frac{2 \sqrt{gh_0}}{1 + \frac{2h}{C} \frac{dC}{dh}}$$

where C is the Chezy coefficient and U_0 , h_0 are uniform flow values of velocity and depth. If C is a constant, then Schönfeld's criterion takes on the form of the Equation (1).

Lighthill and Whitham⁽²¹⁾ introduced the concept of the kinematic wave, one which arises from a functional relationship between discharge and concentration (quantity per unit distance). Comparison of the kinematic wave with the dynamic wave, where Newton's second law of motion governs, also led to a Froude number of two as critical in the case of Chezy resistance. Lighthill and Whitham obtained a critical Froude number of $3/2$ for Manning resistance as did Dressler.⁽⁴⁾

Other investigators⁽⁹⁻¹⁸⁾ have worked on the instability problem, both analytically and experimentally. The formulation of the laminar flow problem has been made by the introduction of perturbations and considerations of the velocity profile.^(15,16) The general problem of a flow with a uniform cross section also has been considered by Craya,⁽¹⁷⁾ Escoffier,⁽¹⁴⁾ and Kuelegan and Patterson.⁽¹²⁾ The results are in agreement with those earlier cited. Craya also obtained the shape correction factor present in Vedernikov's work.

III. PHYSICAL EXPERIMENTS

Minimum physical experimentation was performed, using the facilities of the Fluids Lab of the University of Michigan.

The flume consisted of a masonite false bottom, placed in an existing flume of 50 ft. length, 1 ft. width and 2 ft. depth. The existing flume was of plexiglass framed by aluminum members. The flume was supported on three screw jacks, linked to an electric motor which thus provided a means of changing slope. The slope attainable on the flume was initially considered inadequate (approximately 4%). The considerable roughness of the plexiglass flume, due to construction methods, was quite unacceptable. Therefore, the masonite false bottom was constructed. The masonite had a slope relative to the plexiglass flume of 6%, making the greatest slope attainable approximately 10%. The length of the false bottom was 25 ft. and the width 11-1/2 inches. Sides of masonite were also constructed to alleviate the roughness problem. The masonite surfaces had all screw holes filled, and the entire channel sanded and varnished to provide a smooth surface. Upstream of the 25 ft. sloping section was a 7 ft. section of masonite flume parallel to the bottom of the plexiglass channel, and thus at a flatter slope than the 25 ft. masonite flume. The transition from the 7 ft. section to the 25 ft. section was abrupt.

Water entered the upstream section from the head box of the 50 ft. plexiglass flume. Metering was performed by a venturi meter in a 2 inch supply line. The meter was calibrated in place by means of a weighing tank. Water was supplied from the constant head tank of the laboratory building.

In order to verify experimentally the criterion of instability, the works of the investigators cited indicate that Froude numbers of two should be obtained in a uniform flow. Measurements in the channel described showed that no Froude numbers as low as two were obtainable for any measurable discharges. Due to the length of the flume, and aggravated by the presence of the abrupt change in slope, uniform flow could not be obtained. Instability was present however, and roll waves were very much in evidence.

Further difficulties became apparent. The width of the flume (11-1/2 inches) was so narrow that the depths required were very small (less than .03 ft.), if roll waves were to occur in the channel. The tilting mechanism, which, while providing varying slope of the channel, caused a twisting of the flume so that the bottom of the channel was seldom level in cross section. This caused a speeding up of the waves in one area of a cross section over another area and resulted in distortion of the wave fronts.

However, several beneficial items resulted from the physical study. Suggestion that one cause of roll waves might be the manifestation of eddies sloughing from a change in slope inspired determination of the point of appearance of roll waves down the channel from the change in slope. By visual observation, the point along the channel was determined at which the roll waves were first noticeable. The position was quite simple to ascertain for the slower velocities where it was quite close to the change in slope. For higher velocities, that is greater discharges, the occurrence of discernible roll wave beginnings was quite

far down the channel. Velocities were easily obtained which were so high that the waves did not appear in the channel length.

The depths at the point of occurrence of the roll waves were measured by a dial gage drive to which was attached a pointed, brass probe. An electrical circuit was made from the probe to an oscilloscope, then to a potential source, and then back to a ground trailing in the water slightly downstream of the probe. When the probe was lowered to touch the moving water, the circuit was completed and a signal registered on the oscilloscope. Then the movement of the probe could be read on the dial gage. In practice, the probe was bottomed on the channel floor, raised above the water surface, and then brought back down to make contact. Due to the turbulence of the stream, the surface presented a very rough, fluctuating aspect quite apart from any roll waves. For this reason the signal on the oscilloscope was a series of pulses, all of the same height but varying in duration when the probe was at some mean depth. A visual time average of the pulses gave a highly reproducible value within several percent of the depth (from comparing that value to that of the cases of no contact and of continual contact).

From the depth measurements so obtained at the position at the onset of the roll waves and from the discharges, the velocities, Froude numbers, and Reynolds numbers with both length from the change in slope and depth as the distance parameters were calculated. Figure 1 is a plot of the "depth" Reynolds number on the abscissa versus the "length" Reynolds number on the ordinate. The result is, in effect, a plot of the depth of the flow at the appearance of the waves versus the

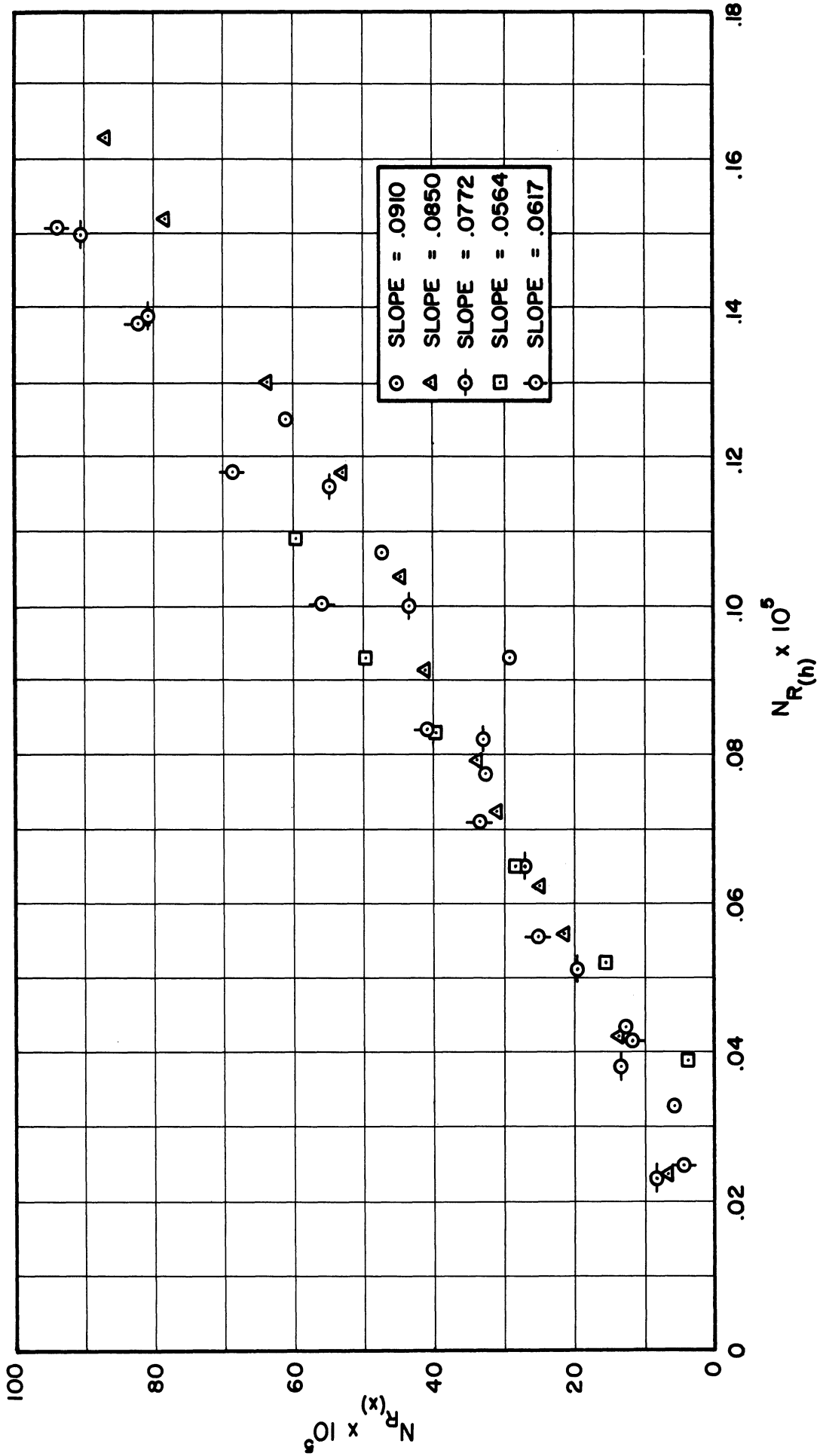


Figure 1. Plot of Depth Reynolds Number Versus Length Reynolds Number for the Occurrence of Roll Waves.

downstream distance from the change of slope of that location. The points show considerable linearity and indicate that the roll waves generated at a common location. The divergence of the points from one another, especially in the larger values, probably reflects observational errors.

Plotting of the Froude numbers against any of the other parameters proved fruitless. This possibly was the result of small variations in the Froude number, and the considerable observational errors.

IV. BASIS FOR COMPUTER METHOD

In order to examine in detail the development of a disturbance introduced into a uniform flow, a finite difference scheme with a specified interval based upon the method of characteristics was used. The method of characteristics has been developed in detail by Courant and Friedrichs.⁽⁷⁾ This discussion will deal with the particular equations pertinent to this study.

The Equations of Flow

The dynamic equation for flow in an open channel is, assuming a uniform velocity distribution,

$$-p_x + \gamma \sin\theta - h_f = \rho(uu_x + u_t)$$

where the positive sense of x , y and u are as indicated in Figure 2

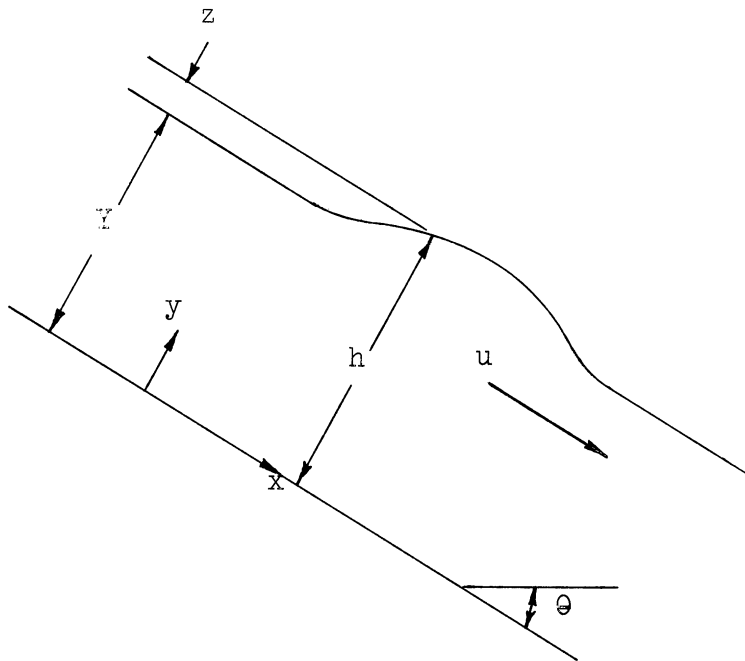


Figure 2. Definition Sketch for Open Channel Flow.

and h_f is a resistance term. The subscripts x and t represent partial differentiation with respect to x and t . If Chezy resistance is introduced and consideration limited to a wide, open-channel, so that the hydraulic radius is approximately equal to the depth, the dynamic equation becomes

$$-p_x + \gamma \sin\theta - \kappa\rho \frac{u^2}{h} = \rho(uu_x + u_t)$$

From Figure 2, a hydrostatic pressure distribution assumption gives,

$$\begin{aligned} p &= \gamma h \cos\theta , \\ &= \gamma(z+Y) \cos\theta , \end{aligned}$$

where Y is uniform flow depth. Then

$$\begin{aligned} p_x &= \gamma z_x \cos\theta , \\ &= \gamma h_x \cos\theta . \end{aligned}$$

Multiplying the dynamic equation by ρ , transposing and making the indicated substitution for p_x ,

$$gh_x \cos\theta - g \sin\theta + \kappa \frac{u^2}{h} + uu_x + u_t = 0 . \quad (2)$$

The equation of continuity is

$$[(uh)_x]dx + (h_t)dx = 0 ,$$

or

$$uh_x + hu_x + h_t = 0 . \quad (3)$$

Introducing the speed of propagation, or the wave speed, c , from a shallow water assumption,

$$c^2 = gh ,$$

and so,

$$\begin{aligned} gh_x &= 2cc_x, \\ gh_t &= 2cc_t. \end{aligned} \tag{4}$$

Substituting Equations (4) into (2) and (3),

$$2cc_x \cos\theta - g \sin\theta + g \frac{\kappa u^2}{c^2} + uu_x + u_t = 0, \tag{2a}$$

$$2uc_x + cu_x + 2c_t = 0. \tag{3a}$$

If the dimensionless variables

$$\bar{x} = \frac{x}{Y}, \quad u = \frac{u}{U}, \quad \bar{c} = \frac{c}{\sqrt{gY}}, \quad \bar{t} = \frac{U}{Y} t$$

are employed (where Y and U are uniform flow depth and velocity), the modified dynamic and continuity equations become,

$$\begin{aligned} 2g\bar{c}\bar{c}_x \cos\theta - g \sin\theta + g\kappa \frac{\bar{u}^2}{\bar{c}^2} \frac{U^2}{gY} + \bar{u}\bar{u}_x \frac{U^2}{Y} + \bar{u}_t \frac{U^2}{Y} &= 0, \\ 2\bar{u}\bar{c}_x + \bar{c}\bar{u}_x + 2\bar{c}_t &= 0. \end{aligned}$$

Writing the Froude number

$$F = \frac{U}{\sqrt{gY}},$$

and dropping the bars on the dimensionless variables for convenience, the equations become

$$\begin{aligned} 2 \cos\theta \, cc_x - \sin\theta + \kappa F^2 \frac{u^2}{c^2} + F^2 uu_x + F^2 u_t &= 0, \\ 2uc_x + cu_x + 2c_t &= 0. \end{aligned} \tag{5}$$

Equations (5) are the nonlinear shallow water equations of flow in a wide, open channel. The shallow water assumption of Equations (4)

requires a large radius of curvature of any variation in height of the depth h . The assumption of hydrostatic pressure distribution is equivalent to the assumption that the vertical acceleration of the flow is negligible. This has been shown by Stoker,⁽⁸⁾ to be correct in the first order as a consequence of the assumption of shallowness.

It is assumed that the resistance to unsteady flow can be represented by values obtained from uniform flow. For uniform flow

$$\sin\theta = \kappa F^2 \frac{u^2}{c^2}$$

in dimensionless quantities. In dimensionless terms, the case of uniform flow is represented by the variable \bar{u} and \bar{c} as

$$\bar{u} = \frac{u}{U} = 1 ,$$

$$\bar{c} = \frac{c}{\sqrt{gY}} = 1$$

(where the bars are again used to denote dimensionless variables). Substituting the values of \bar{u} and \bar{c} into the result of the assumption of applicability of uniform flow resistance,

$$\kappa = \frac{\sin\theta}{F^2} \tag{6}$$

Substitution of (6) into the dynamic equation then gives, along with the equation of continuity,

$$2 \cos\theta \, cc_x - \sin\theta \left(1 - \frac{u^2}{c^2}\right) + F^2 uu_x + F^2 u_t = 0 , \tag{7}$$

$$2uc_x + cu_x + 2c_t = 0 .$$

Equations (7) then are the equations for study. They are called quasi-linear partial differential equations of the first order for functions of two independent variables by Courant and Friedrichs.(7)

The Method of Characteristics

Equations (7) are a system of the hyperbolic type, and as such are amenable to solution by the method of characteristics. To this end we make a linear combination of the Equations (7), viz.,

$$2 \cos\theta \, c c_x - \sin\theta \left(1 - \frac{u^2}{c^2}\right) + F^2 u u_x + F^2 u_t \\ + 2\lambda u c_x + \lambda c u_x + 2\lambda c_t = 0 .$$

Rewriting the combination,

$$\left(\frac{c \cos\theta}{\lambda} + u\right) 2\lambda c_x + 2\lambda c_t + \left(\frac{\lambda c}{F^2} + u\right) F^2 u_x \\ + F^2 u_t - \sin\theta \left(1 - \frac{u^2}{c^2}\right) = 0 . \tag{8}$$

Recognizing

$$\frac{du}{dt} = \frac{\partial u}{\partial x} \frac{dx}{dt} + \frac{\partial u}{\partial t} ,$$

and

$$\frac{dc}{dt} = \frac{\partial c}{\partial x} \frac{dx}{dt} + \frac{\partial c}{\partial t} ,$$

Equation (8) can be written

$$F^2 \frac{du}{dt} + 2\lambda \frac{dc}{dt} - \sin\theta \left(1 - \frac{u^2}{c^2}\right) = 0 . \tag{9}$$

This equation involves the derivatives of u and c in only one direction

(in an x-t plane) when the direction is given by

$$\frac{dx}{dt} = \frac{c \cos\theta}{\lambda} + u ,$$

and

$$\frac{dx}{dt} = \frac{\lambda c}{F^2} + u .$$

Equating values of $\frac{dx}{dt}$,

$$\lambda = \pm F \sqrt{\cos\theta} .$$

So the characteristic directions are given by

$$\frac{dx}{dt} = u + \frac{\sqrt{\cos\theta}}{F} c , \tag{10}$$

$$\frac{dx}{dt} = u - \frac{\sqrt{\cos\theta}}{F} c ,$$

and the characteristic equations become from Equation (9)

$$\frac{du}{dt} + \frac{2\sqrt{\cos\theta}}{F} \frac{dc}{dt} - \frac{\sin\theta}{F^2} \left(1 - \frac{u^2}{c^2}\right) = 0 \tag{11}$$

$$\frac{du}{dt} - \frac{2\sqrt{\cos\theta}}{F} \frac{dc}{dt} - \frac{\sin\theta}{F^2} \left(1 - \frac{u^2}{c^2}\right) = 0 .$$

Notice that the derivatives of u and c appear as total derivatives of t .

Mention should be made here that the choice of dependent variables, or the choice of parameters for non-dimensionalizing is not the only one that can be made. For example, if the dependent variables u and h had been chosen, the equations corresponding to (10) and (11)

would be

$$\frac{dx}{dt} = u + \frac{\sqrt{h \cos\theta}}{F} ,$$

$$\frac{dx}{dt} = u - \frac{\sqrt{h \cos\theta}}{F} ,$$

$$\frac{du}{dt} + \frac{1}{F} \sqrt{\frac{\cos\theta}{h}} \frac{dh}{dt} - \frac{\sin\theta}{F^2} \left(1 - \frac{u^2}{h}\right) = 0 ,$$

$$\frac{du}{dt} - \frac{1}{F} \sqrt{\frac{\cos\theta}{h}} \frac{dh}{dt} - \frac{\sin\theta}{F^2} \left(1 - \frac{u^2}{h}\right) = 0$$

in dimensionless terms. Uniform flow conditions for this case would be

$$\bar{u} = 1, \quad \bar{y} = 1 .$$

Similarly, if the relation

$$\bar{c} = \frac{c}{U}$$

had been the choice to make Equations (2a) and (3a) dimensionless, the result would have been

$$\frac{dx}{dt} = u + c \sqrt{\cos\theta} ,$$

$$\frac{dx}{dt} = u - c \sqrt{\cos\theta} ,$$

$$\frac{du}{dt} + 2\sqrt{\cos\theta} \frac{dc}{dt} - \frac{\sin\theta}{F^2} \left[1 - \frac{u^2}{c^2}\right] = 0 ,$$

$$\frac{du}{dt} - 2\sqrt{\cos\theta} \frac{dc}{dt} - \frac{\sin\theta}{F^2} \left[1 - \frac{u^2}{c^2}\right] = 0 ,$$

with uniform flow conditions of

$$\bar{u} = 1, \quad \bar{c} = \frac{1}{F} .$$

The particular set of equations used would seem to be merely a matter of choice, except perhaps for the last case, where, for uniform flow, the ratio

$$\frac{\bar{u}}{\bar{c}} = F .$$

This case could be considered to represent the dimensional flow more correctly on a descriptive basis, since

$$u = U, \quad h = Y, \quad c = \sqrt{gY}$$

in dimensional terms, and

$$\frac{u}{c} = \frac{U}{\sqrt{gY}} = F .$$

Equations (10) and (11) are a system whereby, in the x-t plane, the direction of the derivatives of u and c in the first of Equations (11) is given by $\frac{dx}{dt}$ of the first of Equations (10); and similarly for the second equations of (11) and (10). Or alternatively, the first of Equations (11) is a constant along a curve represented by the first of Equations (10); and similarly for the second equations. The first equations of (11) and (10) correspond to the "forward" direction of calculation, while the second equations correspond to the "backward" direction. The curves described by the Equations (10) are called the

characteristic curves. If values of u and c are prescribed on a non-characteristic curve Γ , see Figure 3, values of u and c

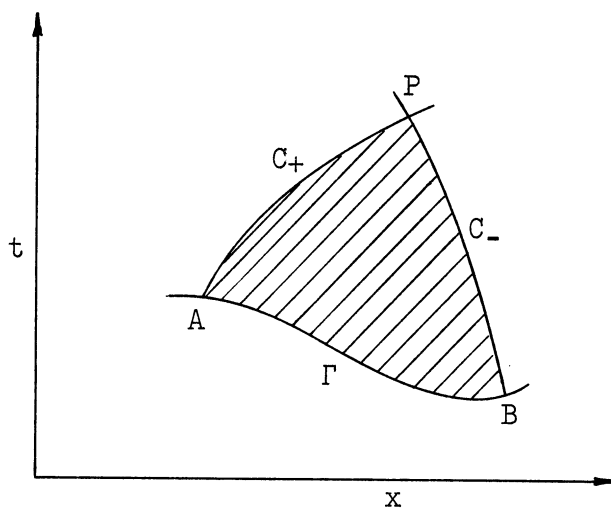


Figure 3. The Characteristic Curves and the Domain of Dependence.

within the area bounded by the characteristic curves C_+ and C_- depend upon those initial values of u and c on Γ between a and B. The values of u and c on the curve Γ outside the interval AB do not affect the computation of u and c within the shaded portion as the disturbances, or variances in u and c are propagated along the characteristic curves of which C_+ and C_- are representative. The characteristic curves C_+ and C_- through point P delineate the domain of dependence AB of the point P. (7)

Similarly, the range of influence of Q on Γ is bounded by the characteristic curves C_+ and C_- through Q, (Figure 4). Unless a shock exists (a bore, or jump, in an open channel flow), characteristic curves of the same "forward" or "backward" direction do not cross on another, so the validity of the domain of dependence is assured.

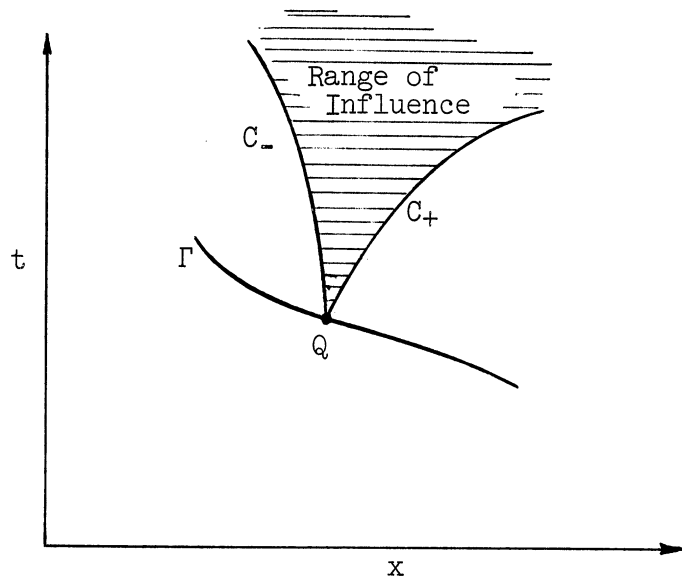


Figure 4. The Range of Influence.

If the values of u and c are known for initial conditions, that is, if

$$u(x,0), \quad c(x,0), \quad L_1 < x < L_2 ,$$

are given, the solution can be computed in the area of the $x-t$ plane bounded by C_+ , C_- and the line $t = 0$, $L_1 < x < L_2$, for that area is the range of influence of L_1L_2 . See Figure 5. If specified finite intervals of x and t are taken in that area, and the intervals are small enough that the characteristic curves emanating from points in L_1L_2 can be represented by straight lines, a method of solution of Equations (7) becomes clear.

Values of the characteristic directions, Equations (10), are computed from known values of u and c at A_1, A_2, \dots . These values of the directions are then used at the corresponding points to be computed, B_1, B_2, \dots , to provide a means for interpolation between points

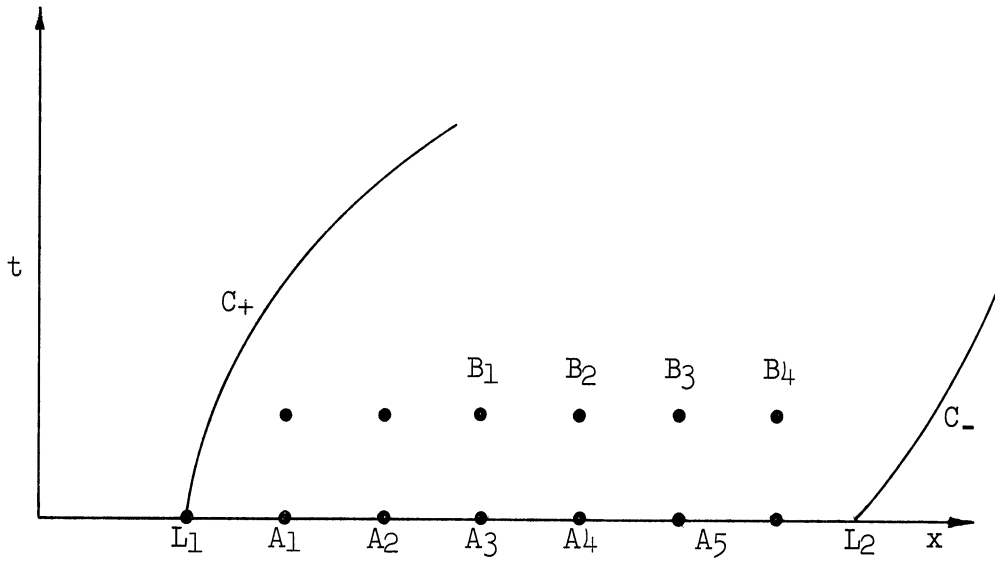


Figure 5. The Range of Influence of a Set of Initial Values.

on the line of A_1, A_2, \dots . Then Equations (11), in a finite difference form, are solved simultaneously for c and u at the point in the next row (of B_1, B_2, \dots). This use of the theory of characteristics has been called a method of specified time intervals by Lister. (19)

The Formulation for the Computer Solution

In the study at hand, the characteristic directions, from Equations (10), are

$$\zeta_+ = u + \frac{c \sqrt{\cos \theta}}{F} ,$$

$$\zeta_- = u - \frac{c \sqrt{\cos \theta}}{F} .$$

For values of u and c close to unity, Froude numbers greater than one, and for moderate slopes,

$$\zeta_+ \cong 1 + \frac{1}{F} = \frac{F+1}{F} > 1 ,$$

$$\zeta_- \cong 1 - \frac{1}{F} = \frac{F-1}{F} < 1 .$$

So if the increments of non-dimensional t and x , Δt and Δx respectively, are equal, the curves C_+ and C_- , of which ζ_+ and ζ_- approximate the slopes, will intersect the line $t = t_1$ of known values as is shown in Figure 6. Then, to calculate the values of u and c at P , the initial values, u_B, c_B , are used to compute ζ_+ and ζ_- , for only point B is in the domain of dependence of P . ζ_+ and ζ_- are used to interpolate for values of u_R, c_R and u_S, c_S , and the values u_R, c_R, u_S, c_S are employed as the initial values for solution of u_p, c_p . To this end, Equations (10) and (11) are written as difference equations using the notation indicated by Figure 6.

$$\begin{aligned}
 (x_P - x_R) - (u_B + \frac{\sqrt{\cos\theta}}{F} c_B)(t_P - t_R) &= 0 , \\
 (x_P - x_S) - (u_B - \frac{\sqrt{\cos\theta}}{F} c_B)(t_P - t_S) &= 0 , \\
 (u_P - u_R) + \frac{2\sqrt{\cos\theta}}{F} (c_P - c_R) - \frac{\sin\theta}{F^2} (1 - \frac{u_B^2}{c_B^2}) &= 0 , \\
 (u_P - u_S) - \frac{2\sqrt{\cos\theta}}{F} (c_P - c_S) - \frac{\sin\theta}{F^2} (1 - \frac{u_B^2}{c_B^2}) &= 0 .
 \end{aligned} \tag{12}$$

Writing ζ_+ and ζ_- for what they are in difference terms, the first two of Equations (12) give,

$$\begin{aligned}
 \zeta_+ &= \frac{x_P - x_R}{t_P - t_R} = u_B + \frac{\sqrt{\cos\theta}}{F} c_B , \\
 \zeta_- &= \frac{x_P - x_S}{t_P - t_S} = u_B - \frac{\sqrt{\cos\theta}}{F} c_B .
 \end{aligned} \tag{13}$$

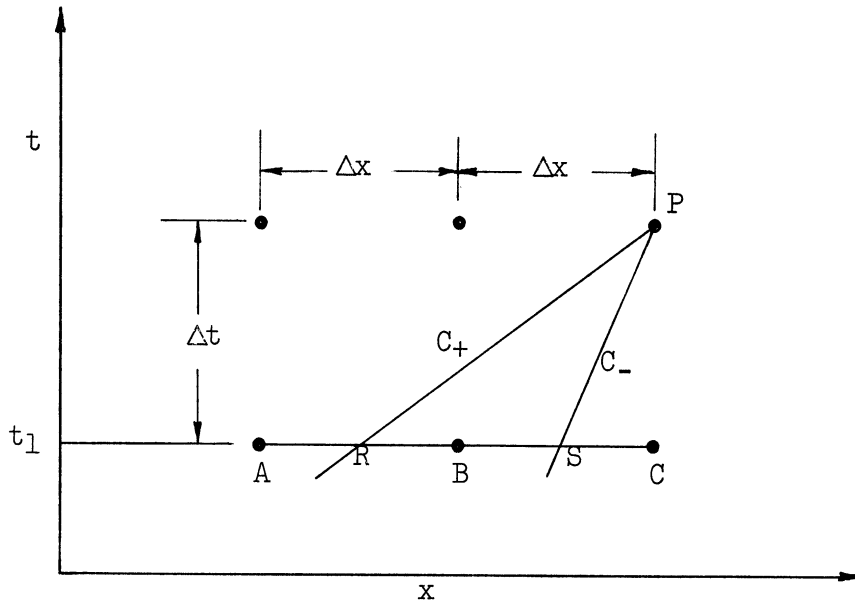


Figure 6. The Intersection of Characteristic Curves and Initial Data.

The values of u_R , c_R , u_S , c_S are now calculated by a linear interpolation using ζ_+ and ζ_- .

$$\frac{1}{\zeta_+} = \frac{\Delta t}{2\Delta x} \cdot \frac{1}{\frac{u_C - u_R}{u_C - u_A}},$$

$$\frac{1}{\zeta_+} = \frac{\Delta t}{2\Delta x} \cdot \frac{1}{\frac{c_C - c_R}{c_C - c_A}},$$

$$\frac{1}{\zeta_-} = \frac{\Delta t}{\Delta x} \cdot \frac{1}{\frac{u_C - u_S}{u_C - u_B}},$$

$$\frac{1}{\zeta_-} = \frac{\Delta t}{\Delta x} \cdot \frac{1}{\frac{c_C - c_S}{c_C - c_B}}.$$

Solution of these equations for the desired values gives,

$$\begin{aligned}
 u_R &= u_C - \zeta_+ \frac{\Delta t}{2\Delta x} (u_C - u_A) , \\
 c_R &= c_C - \zeta_+ \frac{\Delta t}{2\Delta x} (c_C - c_A) , \\
 u_S &= u_C - \zeta_- \frac{\Delta t}{\Delta x} (u_C - u_B) , \\
 c_S &= c_C - \zeta_- \frac{\Delta t}{\Delta x} (c_C - c_B) .
 \end{aligned}
 \tag{14}$$

Solving the last two of Equations (12) simultaneously for u_P and c_P , (after first recognizing $(t_P - t_R) = (t_P - t_S) = \Delta t$).

$$\begin{aligned}
 u_P &= \frac{1}{2} (u_R + u_S) + \frac{\sqrt{\cos\theta}}{F} (c_R - c_S) + \frac{\sin\theta}{F^2} \left(1 - \frac{u_B^2}{c_B^2}\right) \Delta t , \\
 c_P &= \frac{F}{4\sqrt{\cos\theta}} (u_R - u_S) + \frac{1}{2} (c_R + c_S) .
 \end{aligned}
 \tag{15}$$

The procedure of computation then is to use known values of u and c to solve for ζ_+ and ζ_- by Equations (13). Using known values of u and c and the values of ζ_+ and ζ_- , Equations (14) are used to find u_R, c_R, u_S, c_S . Then Equations (15) are applied to calculate u_P, c_P . In such a fashion, values of u and c can be computed ranging over the entire area shaded in Figure 5. The solution thus found converges to the true solution as the mesh size of $\Delta t, \Delta x$ reduces to zero, or as $\Delta t \rightarrow 0, \Delta x \rightarrow 0$.

In general, if the functions $u(L_1, t), c(L_1, t), u(L_2, t), c(L_2, t), u(x, 0), c(x, 0)$ for $L_1 < x < L_2$, are known, then the computation can proceed through the entire domain $t > 0, L_1 < x < L_2$

(see Figure). In the present problem, the "backward" characteristic curve, C_- , in reality has a positive slope. Any values of c and u to the left of C_+ in the $x-t$ plane (Figure 5) would have to be continuous with values of c and u inside the shaded region. If the values were not continuous, the discontinuities themselves would be disturbances which would be propagated into the flow, and would tend to distort the wave shape changes. For this reason, and because of the difficulty in attaining continuous variables across C_+ , it is better to compute from the C_+ curve. In other words, to compute only in the range of influence of initial values of the form

$$\begin{aligned} u &= u(x,0) , \\ c &= c(x,0) , \end{aligned} \quad L_1 < x < L_2 .$$

The computations were performed on an IBM 709 digital computer at the Computing Center of the University of Michigan. The Computing Center has developed a machine language for use on its 709 equipment called the Michigan Algorithm Decoder, or MAD. The program designed to perform the computations was written in the MAD language, and is reproduced in the Appendix. The variable notation in the program follows that used in this thesis as far as is possible. The various major portions of the program are labelled for guidance.

Variation of several parameters was permitted; they were:

- Froude number (F),
- Slope (SL),
- Maximum amplitude of disturbance (A),
- Wave length (WL),
- Exponential decay factor (Kl).

The first two parameters, the Froude number and slope, defined a flow. The second two, the maximum amplitude and wave length, permitted variations so that a large radius of curvature of the surface relative to the magnitude of the disturbance was assured. The last, the exponential decay factor, permitted changing the amplitude downstream so that the effect of different wave heights on one another could be observed. It was thought that a change of wave length might result from differences in wave height.

The disturbances introduced were generated by the part of the program called the external function. The disturbances were sinusoidal variations of the depth, with the exponential term to permit a change of depth along the stream, thus in dimensionless terms,

$$h = 1 + A \exp(-Kl \cdot x) \cdot \sin\left(\frac{2\pi x}{WL}\right) .$$

Initial values of c and u were computed from the depth for various values of x by

$$c = \sqrt{h} , \quad (\text{wave speed in shallow water}),$$

$$u = \frac{1}{h} , \quad (\text{continuity}) ,$$

again in dimensionless variables.

The results of computation were printed for every time increment. Lists were printed of all the velocities, then all the wave speeds, then depths, and finally the corresponding x -distances to the locations of the results. Prior to the printing of the lists a general

heading for each set of variables was printed, along with the flow parameters. An example of the output is shown in the Appendix.

The results obtained from the computer were plotted, the features chosen as most representative being the depth and velocity.

The Convergence of the Solution

The method as presented gave accuracy only in the first order of the dimensions of the mesh. Higher orders of accuracy could have been obtained by extrapolation methods, as developed by Lister.⁽¹⁹⁾ The extrapolation methods for second order accuracy would have required twice the variable storage. Three cycles of computation in the computation block would have been necessary plus computation of an extrapolation formula. This would have meant somewhat more than five times the computer time required for first order accuracy. Note that dimensional time

$$t = \frac{Y}{U} \bar{t}$$

by definition of dimensionless time \bar{t} . For this study

$$\frac{U^2}{128.8} > Y$$

in nearly all cases, because $F > 2$. Therefore

$$t < \frac{U}{128.8} \bar{t} .$$

Then, in a real flow case, where U might be approximately 2.5 feet/second, the dimensional time corresponding to a non-dimensional time of unity would be about .02 seconds. For that reason, saving of computer

time was highly desirable, since twenty cycles through the computation and output blocks took the IBM 709 about twelve minutes. For the time increment chosen, the twenty computation cycles would have resulted in a total non-dimensional time of 2. Greater accuracy could also have been attained by reduction in mesh size, but for the same reasons, the degree of this reduction was limited.

The problem of staying in the range of influence of the initial data was met by dropping the upstream two points after each computation cycle. This was accomplished in the program by means of incrementing the index integer labelled J. The effect of the point which is most upstream in the row of known values, reaches only the third point in the row being computed, hence computation of the third point and all subsequent points can be made without fear of introducing an unwanted disturbance. No points other than the first two in the row of known values are involved in the computation of the third point of the row being computed. This condition is assured by the interpolation formulas for u_R and c_R involving ζ_+ . When computation in the next row is begun, that which was the third point in the preceding row is now the first point in the newly computed row of known values, and the argument is repeated.

As the changes in value of u and c develop, it is possible that the intersection of C_+ and C_- with the row of known values will fall outside the predicted intervals. It would be quite possible to expand the computer program to encompass this condition, but several obstacles arise. First, the program would become quite a bit more complex,

with all the attendant difficulties of clearing errors, checking for accuracy of logic, and so on. Second, the computation time would have been increased, since for each point a check of the intersection would have to be made and corrections performed before computation could be made at the point. An increase in variable storage would also be needed, but this probably could be kept at a minimum and would not be a factor. Because of the demand of these obstacles upon computing time, no attempt was made to improve the interpolation approximation. It is considered that such an omission is not a major source of error. This is because the interpolation is an approximation; the point of interception will not be far from the interval predicted; and the interpolation formulas hold even when the point of interception is outside the interval.

V. RESULTS OF COMPUTER COMPUTATION

The results of the computer calculation were plotted to facilitate observation. Partial results of the plotting appear in Figures 7 to 14.

The features chosen for plotting were non-dimensional depth and flow velocity versus length down the channel. Depth and velocity are measured along the ordinate, while channel length is measured along the abscissa. The vertical scale is magnified twenty times with respect to the horizontal scale. The curve of depth is a solid line, while that of velocity is dashed.

Each set of curves represents the evolution with time of depth and velocity for a certain set of the parameters governing the flow and wave size. These parameters label each set of curves. The symbols representing the parameters are:

F, Froude number;

SL, Slope;

Kl, Exponential decay factor;

WL, Wave length;

A, Maximum wave amplitude.

The non-dimensional time of occurrence accompanies each pair of depth and velocity curves.

Since all the curves represent the results of data which included a decay factor other than zero, the curves of the initial disturbance show a reduction in magnitude along the channel length. Because of the requirement of dropping the first two points of computation

in each row, the plotting was performed at various downstream channel locations, depending upon the total time the problem was generated in the computer. Accordingly, the initial data of various sets of parameters show different amplitudes.

Some general comments can be made about the curves:

1. All the surface profiles exhibit a tendency for the upstream side of the wave to steepen more than the downstream side. That is, the distance along the channel, going downstream, from trough to crest is less than the distance from crest to trough. Schönfeld⁽⁶⁾ indicates that the upstream side of a disturbance will steepen and then begin to flatten. No upstream flattening is apparent in these profiles.
2. The wave lengths of the disturbances do not show any change. This is true despite variation of any of the parameters describing the flow or the disturbance.
3. A pulsation, or beat, occurs in the velocity and depth. This pulsation is best seen in those sets of curves which are for the larger times, but the beginning can be noticed in most of the others.
4. The variations of depth and velocity tend to stay about 90 degrees out of phase. When the depth variations are greatest, the velocity curve has experienced its greatest phase shift relative to the depth curve. When the depth variations have lessened the phase of the velocity curve relative to the depth curve is again near 90 degrees.

The pulsation of the amplitudes of both depth and velocity variations appears to be the result of the reciprocal nature of the depth and velocity in the initial disturbance. The fluid particles in the shallower depths are carried along faster by the higher velocities, while particles in the greater depths are moving more slowly relative to a reference velocity. This results in a piling up of fluid, and a lessening of velocity variation. When the velocity variation is no longer sufficient to support further growth of depth variations, dispersion of the wave begins, and causes a reduction in wave height along with an increase in velocity variation. This reduction continues until a period of renewed growth begins. The eventual changes in and role of the pulsations must be a subject for further study employing much longer effective computing times. The only observation that can be made of the pulsations is that the period of pulsations seems to be longer for cases of greater depth variations, in general, higher Froude numbers.

A test of the validity of the method must be concerned with stability and Froude number. For the equations at hand, Dressler's instability criterion⁽⁴⁾ can be written as

$$F > 2\sqrt{\cos\theta}$$

assuming uniform flow can be used to evaluate the resistance coefficient. For the slope most commonly used in the graphs,

$$\sqrt{\cos\theta} \cong 1 .$$

Therefore, a flow with $F = 1.5$ should be stable, one with $F = 3$ should be unstable. Figure 11 represents flow with $F = 1.5$, Figure 7 represents flow with $F = 3$.

The flow with $F = 1.5$, $A = .05$ (Figure 11) shows a definite tendency for the amplitude of the waves to decrease after an initial period of growth. This period of growth ends at approximately time 1.5, and then a decrease begins which continues until time 3.0. At time 3.0, a new cycle starts which has not yet reached a low point at time 5.5. This observation is based upon the shape of the profiles at time 5.5 which are quite similar, except for amplitude, to those of time 2.5. On the other hand the profiles of time 3.0, where the decrease of the heights of the waves momentarily are halted, show a pattern of rise and fall similar to the initial disturbance of time 1.0. It could be expected that the pulsation will be repeated, and such is the case, with an increase in variation to time 4.0, and then a decrease to about time 6.0. The wave heights at time 4.0, which represents the peak of the second period of growth, show a maximum amplitude nearly exactly that of the initial disturbance. This is considered to be a coincidence.

Flow with $F = 3$ should show a growth in wave heights leading eventually to a discontinuous water surface, or breaking of the waves. Prior to that point, it is expected that the assumption of no vertical acceleration would become invalid, and that the intersection of the characteristic curves with the line of computed data would fall so far outside the interval assumed that the interpolation made there

would have little merit. Profiles of velocity and depth for $F = 3$, $A = .05$ (Figure 7) show a rapid growth of depth variation, and a corresponding decrease in variation of velocity up to time 2.5. Then there is a decline in the amplitude of the waves until time 6.0, when a period of considerable growth begins again.

The question is whether the flow is unstable for $F = 3$. Figure 7 does not offer conclusive proof of instability, but there are differences between the curves for $F = 3$ and $F = 1.5$ which indicate instability.

1. The first increase in depth variation for $F = 3$ is much greater relative to the initial disturbance than the increase in depth variation for $F = 1.5$.
2. A considerable increase in depth variation continues for a longer time for the higher Froude number.
3. The time of maximum decline of amplitude, time 6.0, for $F = 3$ still exhibits amplitudes of the same magnitude as the original disturbance.

These differences can lead to a conclusion that the flow is unstable for a Froude number of 3, but a definite statement would require a much longer period of computation. This must wait for the advent of a faster computer.

Opposing the instability conclusion is the fact that the second increase in depth variation in the case of $F = 3$, which occurs at time 8.5 shows less variation in depth and velocity than time 2.5. This could be the result of another pulse or beat with a still longer

period than the first, which has a non-dimensional period of about 3.0. A longer computation would also resolve this question.

Other curves support the instability conclusion. Figure 10 shows the development for a short time of flows with $F = 3$ and $F = 4$ for comparison. The initial disturbances are identical, with a maximum amplitude of 0.05. The flow with $F = 4$ shows considerably more variation than the flow with $F = 3$, which would indicate a higher degree of instability.

Figure 9 represents the state of the flow for $F = 2.5$ and $A = .1$. It is to be expected that the larger maximum amplitudes (values of A) would cause an earlier indication of instability. Figure 9 shows an extremely large increase in variation of depth up to time 2.0, then a decrease to an extremely distorted pattern at time 5.5, where the depth variations are still of almost the same magnitude as those of the initial disturbance. This condition gives evidence of continued instability.

Figure 12 is for the case of $F = 1$, $A = .1$, $SL = .1$. This case was computed because the intersections of the characteristic curves with the line of known points would not be very far outside the assumed intervals. A decline in the depth variation is evident. Also of interest is the fact that the wave does not progress down the channel as is the case with the flows of $F > 1$. What would happen to the profiles after time 4.0 is conjecture, but it appears that the wave is being dispersed by a drawing out of the fluid on the downstream side of the wave.

The effect of sharply decreasing the amplitude of successive waves by increasing the decay factor is shown in Figure 13. Any

expectation of the larger waves overtaking smaller waves is fruitless, as the interval from crest to crest remains the same. Development of roll waves by incorporation of smaller, slower waves by larger, faster waves must not occur until the assumptions governing Equations (7) are invalid.

Figure 8 shows the development of the disturbance for consecutive time intervals used in computer computations. This figure serves to illustrate the changes occurring between time 0. and time 0.5 which the other figures omit.

The effect of changing the slope is illustrated by Figure 14. The depth variation resulting in the case of shallower slope are greater than the depth variations when the slope is steeper. Comparison of Figure 14 and Figure 7 illustrates the condition. Thus, a particular Froude number in the unstable range for a given slope represents a higher degree of instability than the same Froude number when the flow is on a steeper slope. As might be expected, the effect of a change is not as great as the effect of a change of Froude number.

VI. CONCLUSIONS

The conclusions of this study are:

1. The method of characteristics can be used to predict the development of disturbances in an unstable supercritical flow within the assumptions made.
2. While the Equations (7) still govern the flow, and the assumptions made are still valid, no change in wavelength of a decaying sinusoidal disturbance is indicated.
3. A pulsation in the variation of depth and velocity with respect to time is noted for all flows investigated.
4. The role of the Froude number as the most significant parameter in instability growth is verified.

Further study is suggested, principally in the shape of disturbances, initial velocity and depth relationships, and in greater non-dimensional times.

FIGURES 7 THRU 14

PLOTS OF THE COMPUTER SOLUTIONS OF NON-DIMENSIONAL
DEPTH AND VELOCITY VERSUS CHANNEL LENGTH
FOR VARIOUS FLOW PARAMETERS

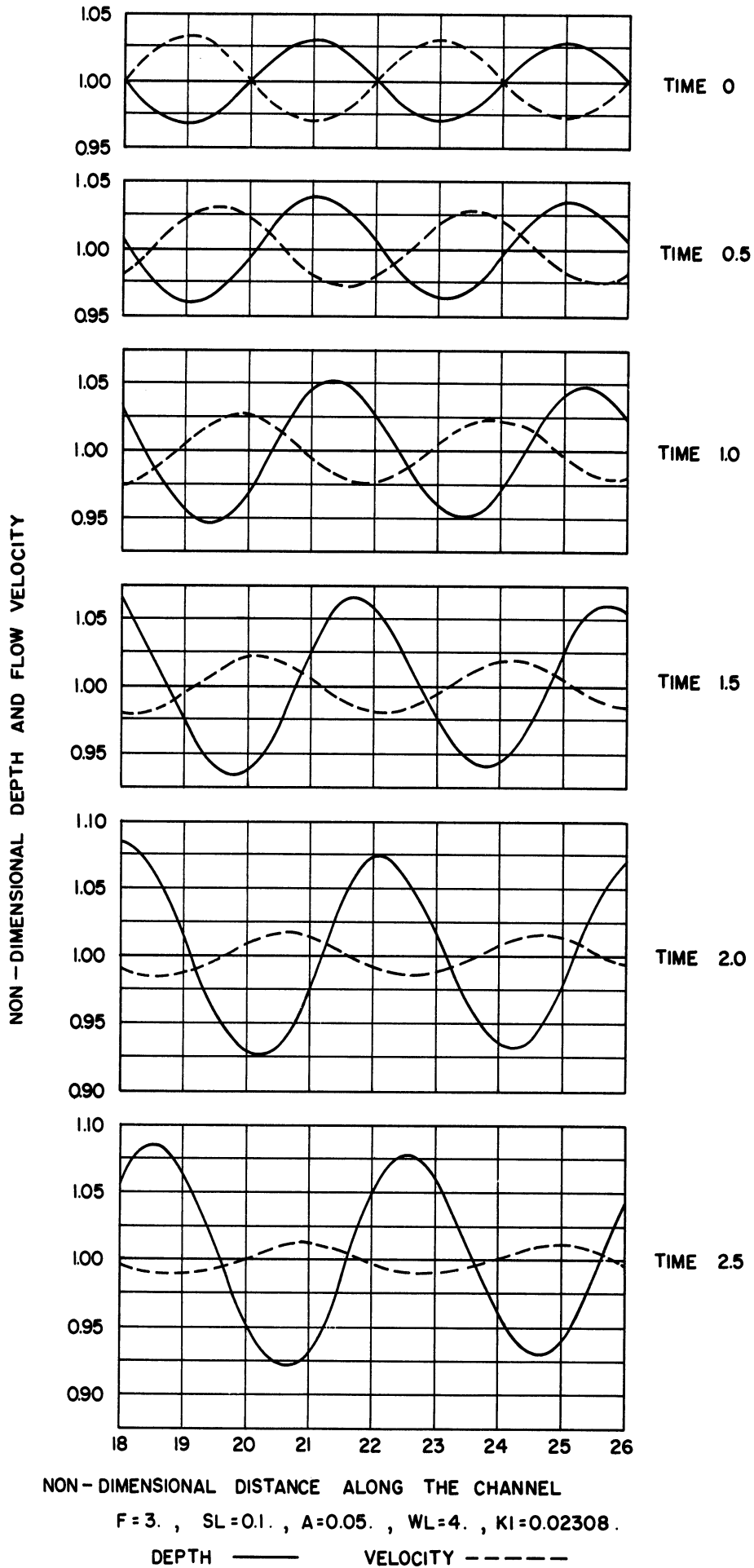


Figure 7a.

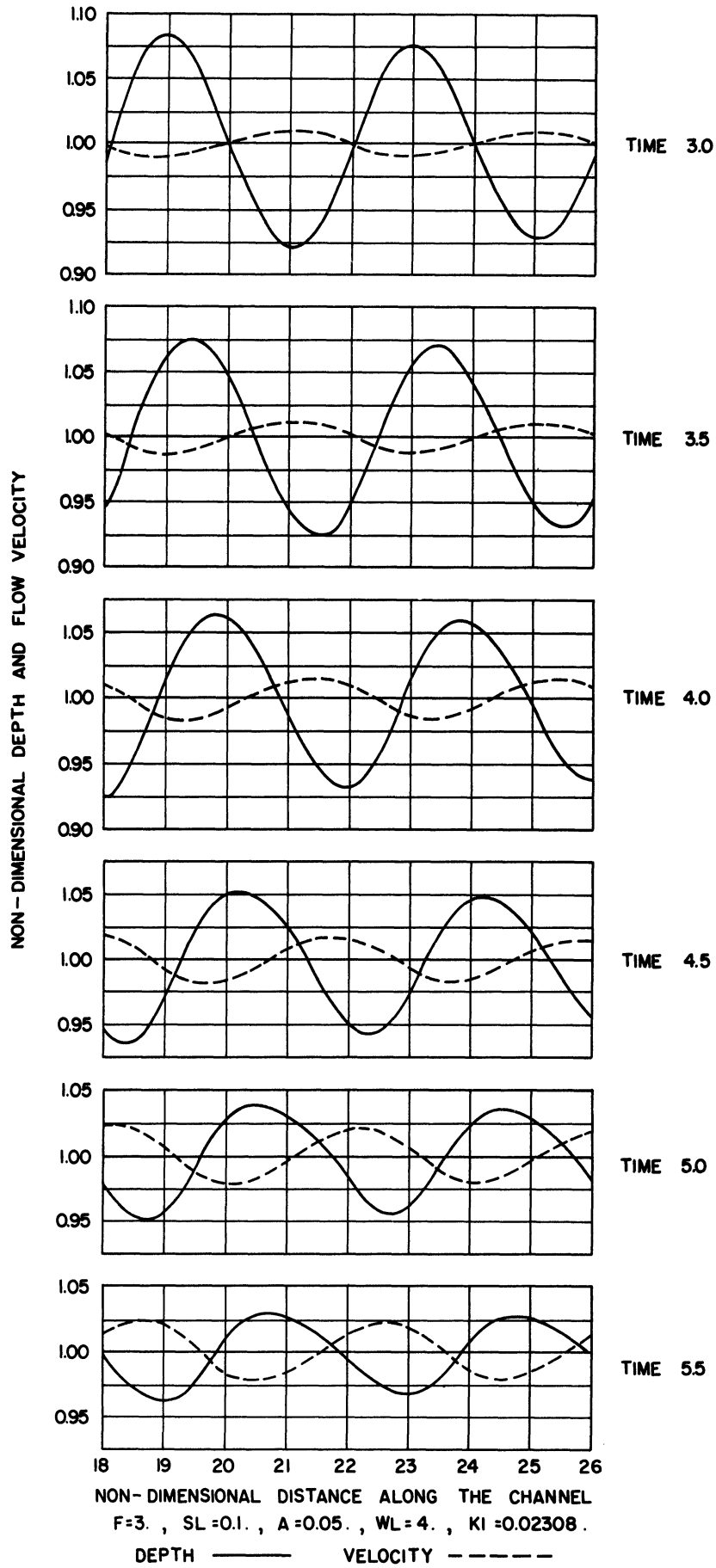


Figure 7b.

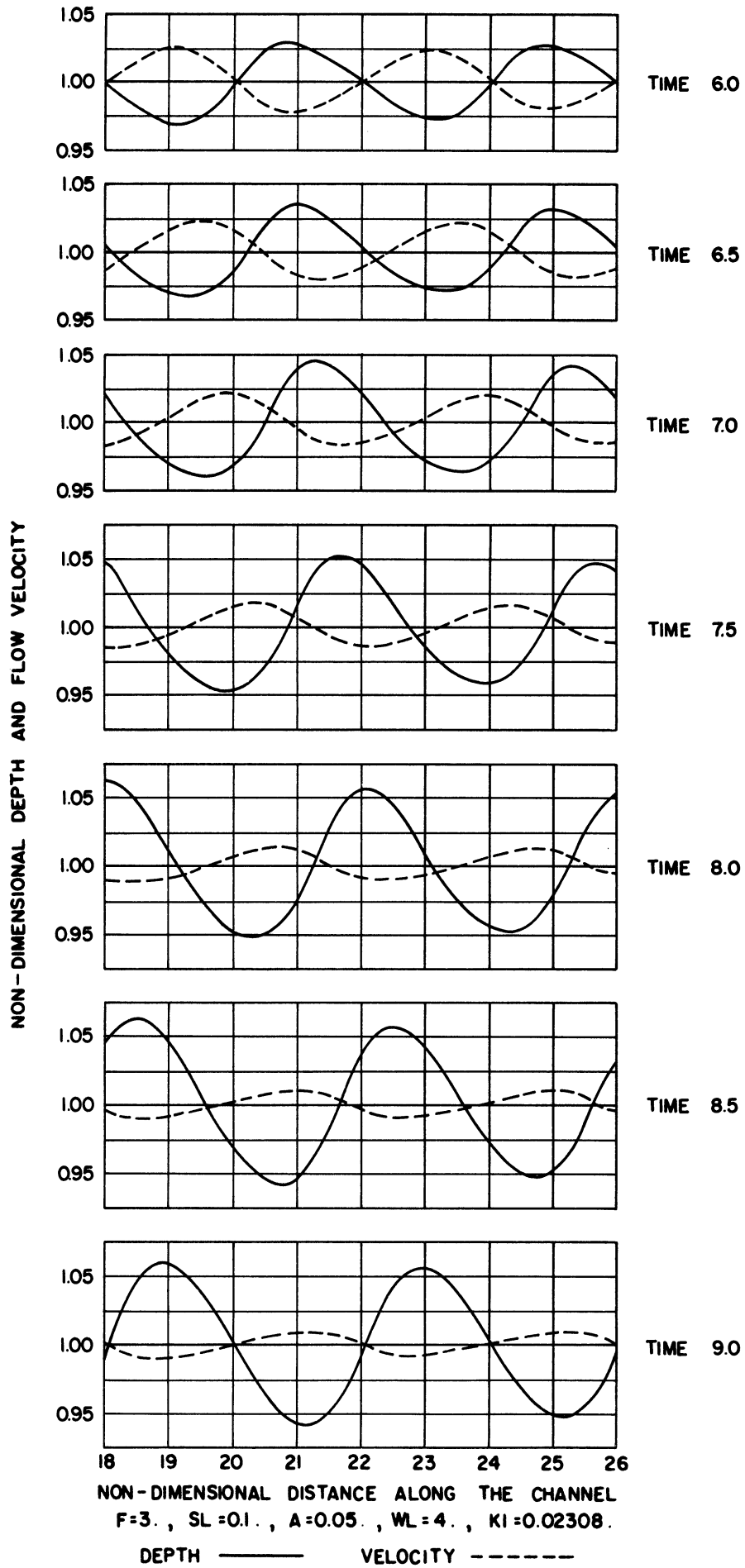


Figure 7c.

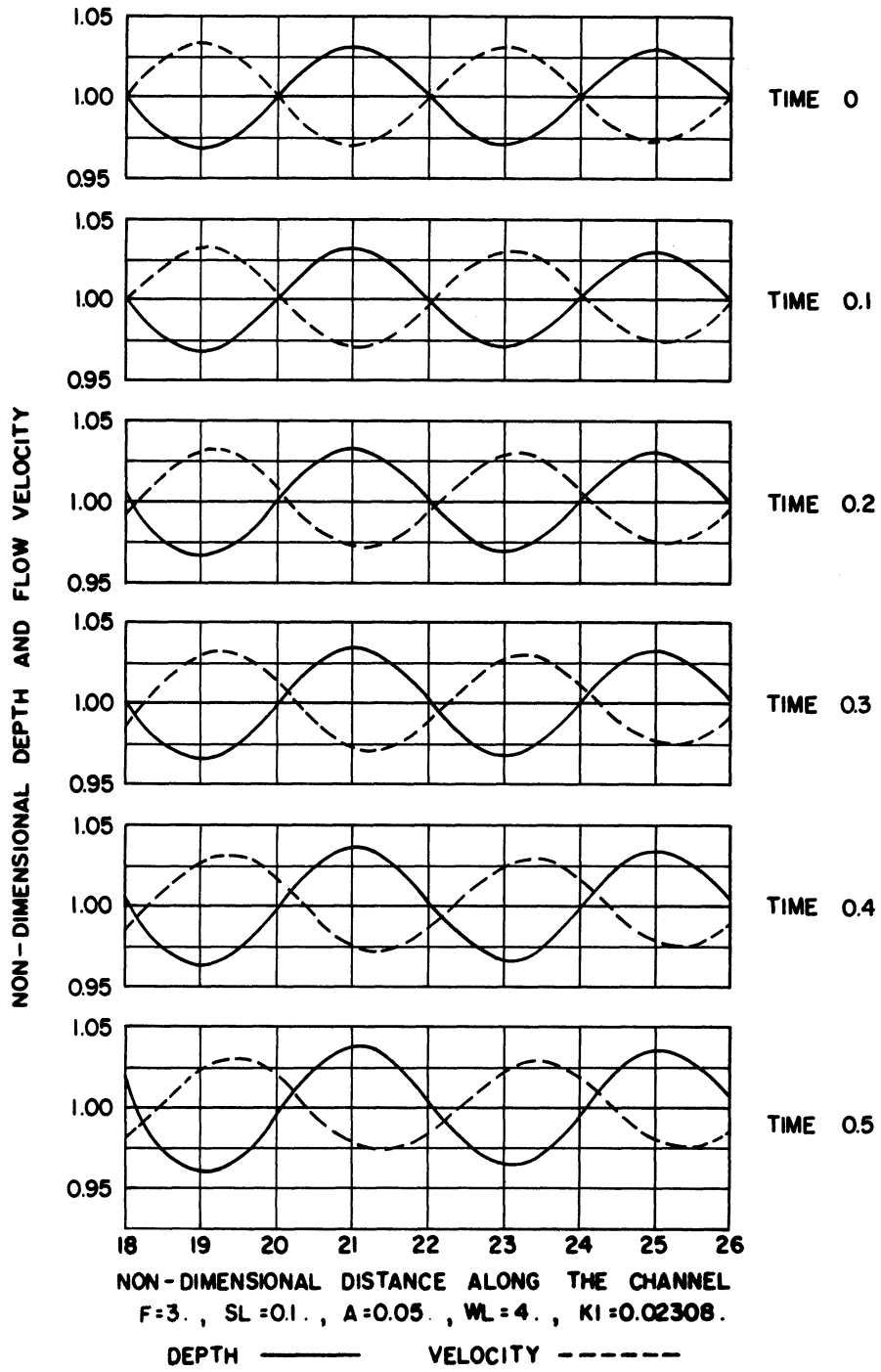


Figure 8.

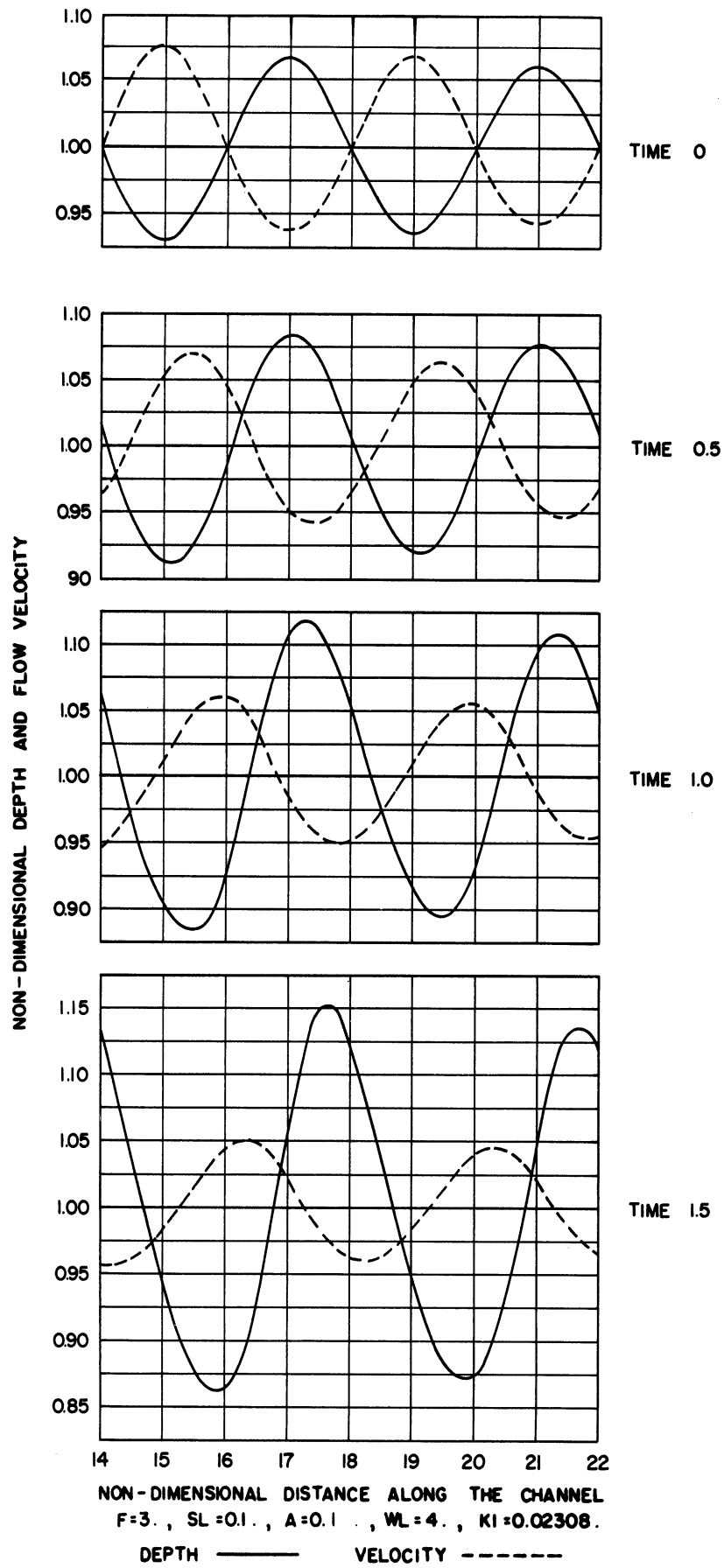


Figure 9a.

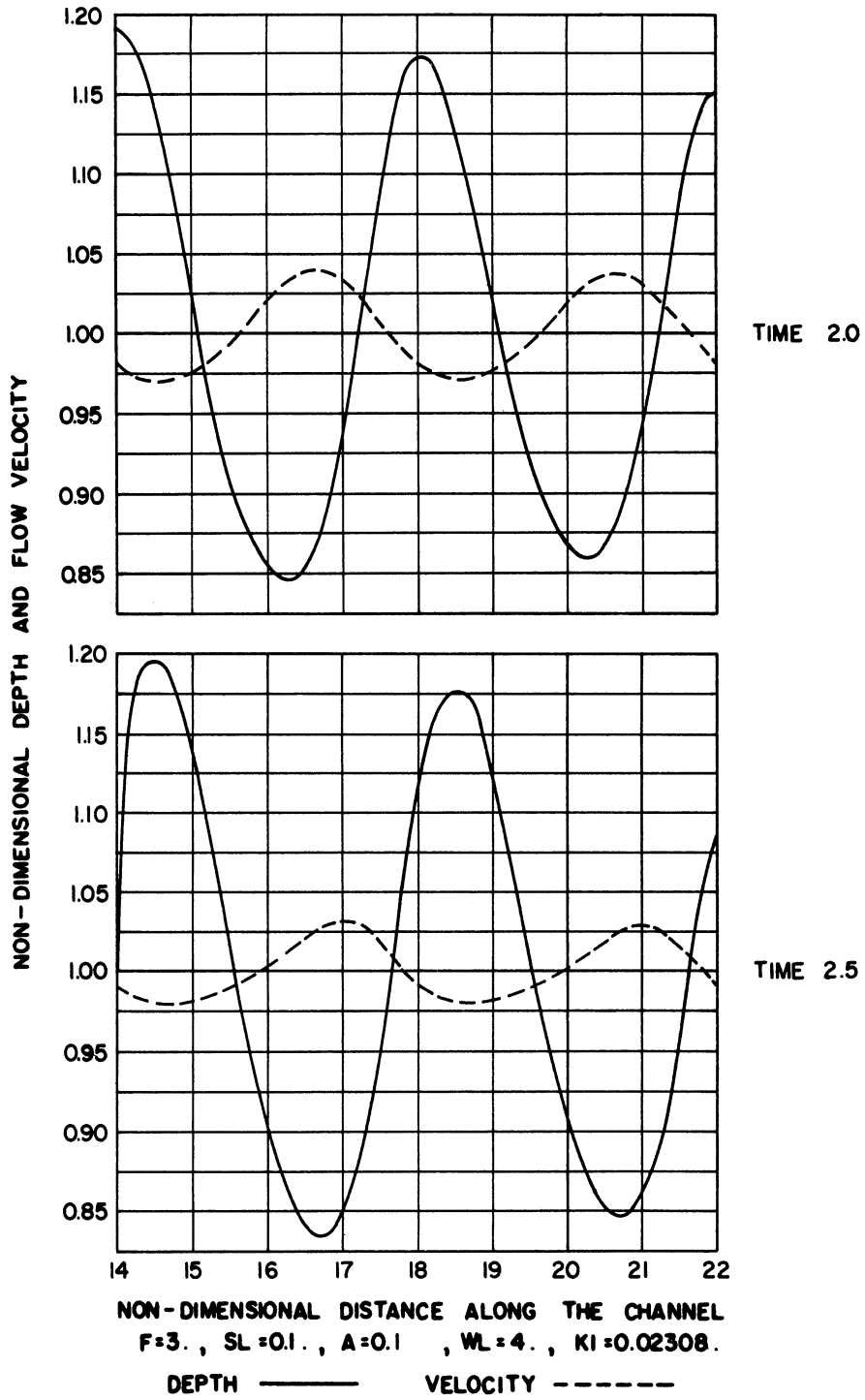


Figure 9b.

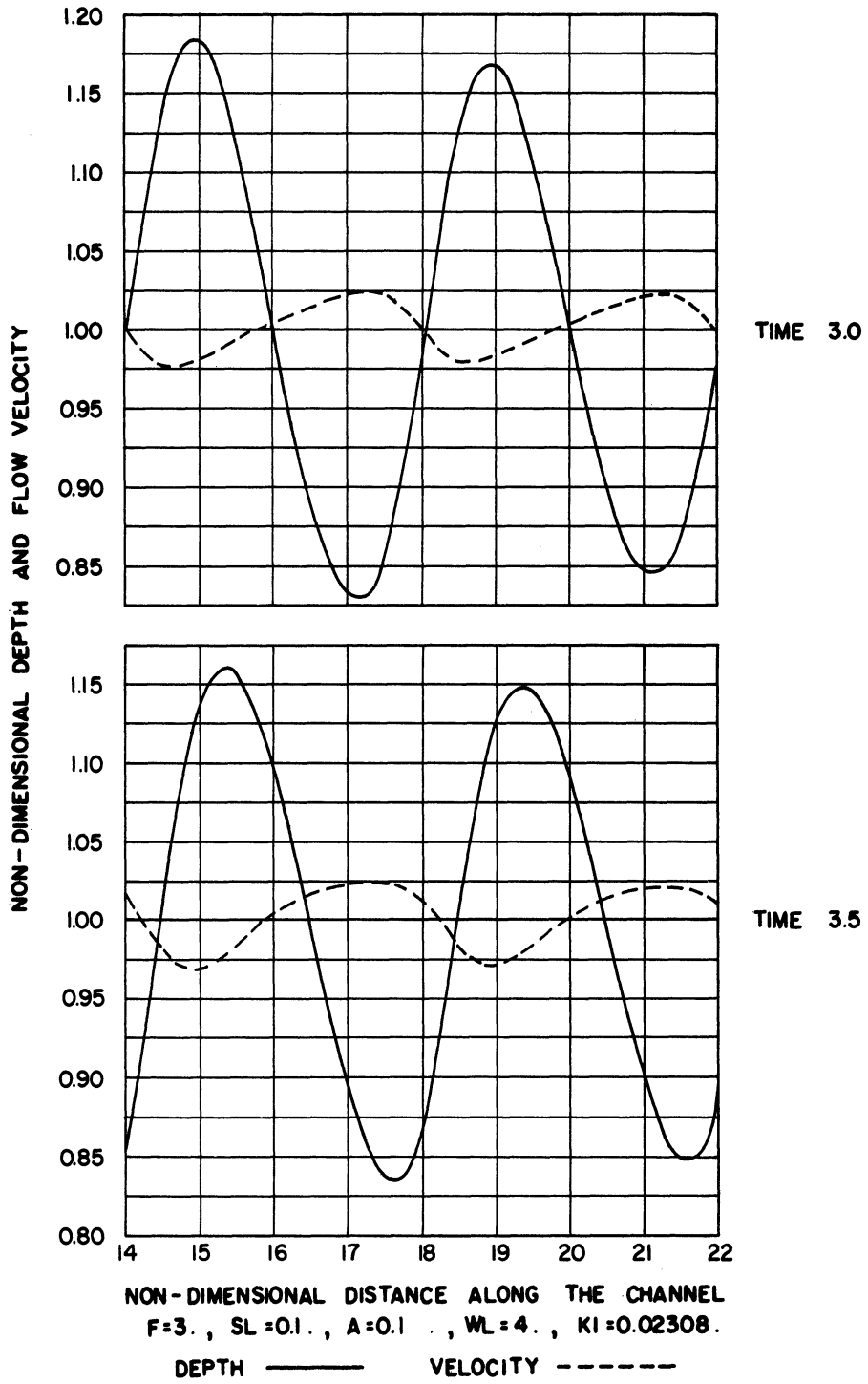


Figure 9c.

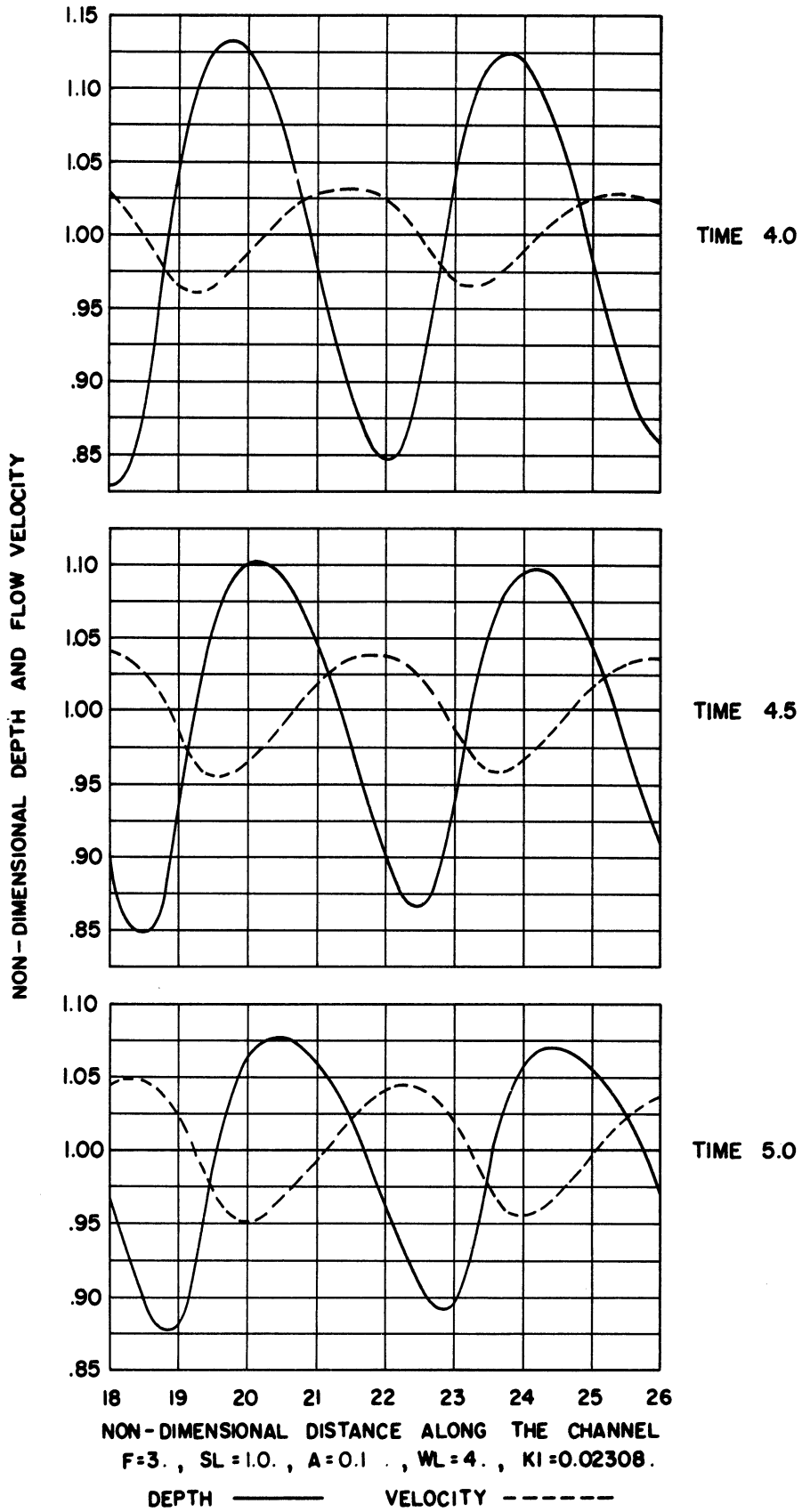


Figure 9d.

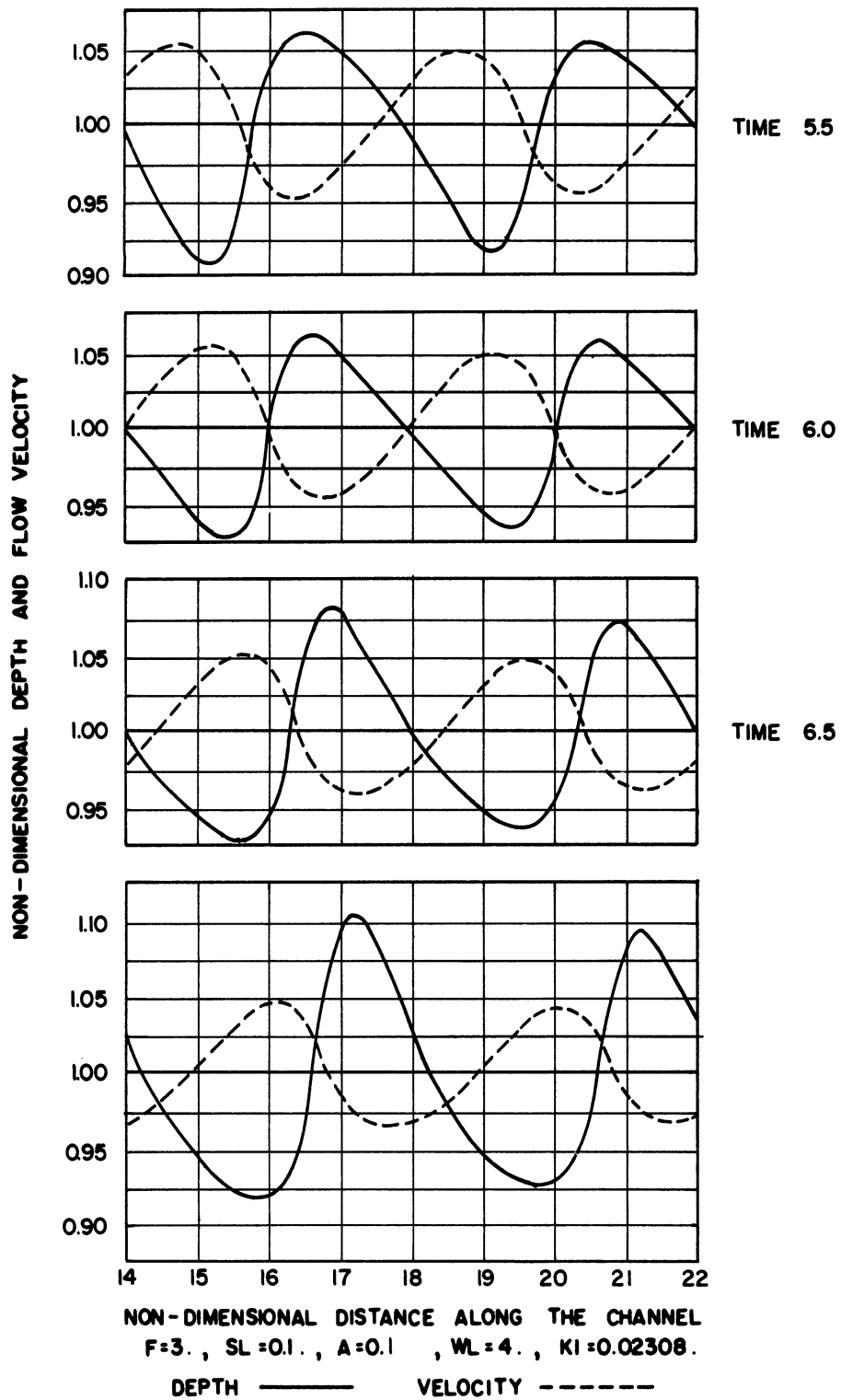


Figure 9e.

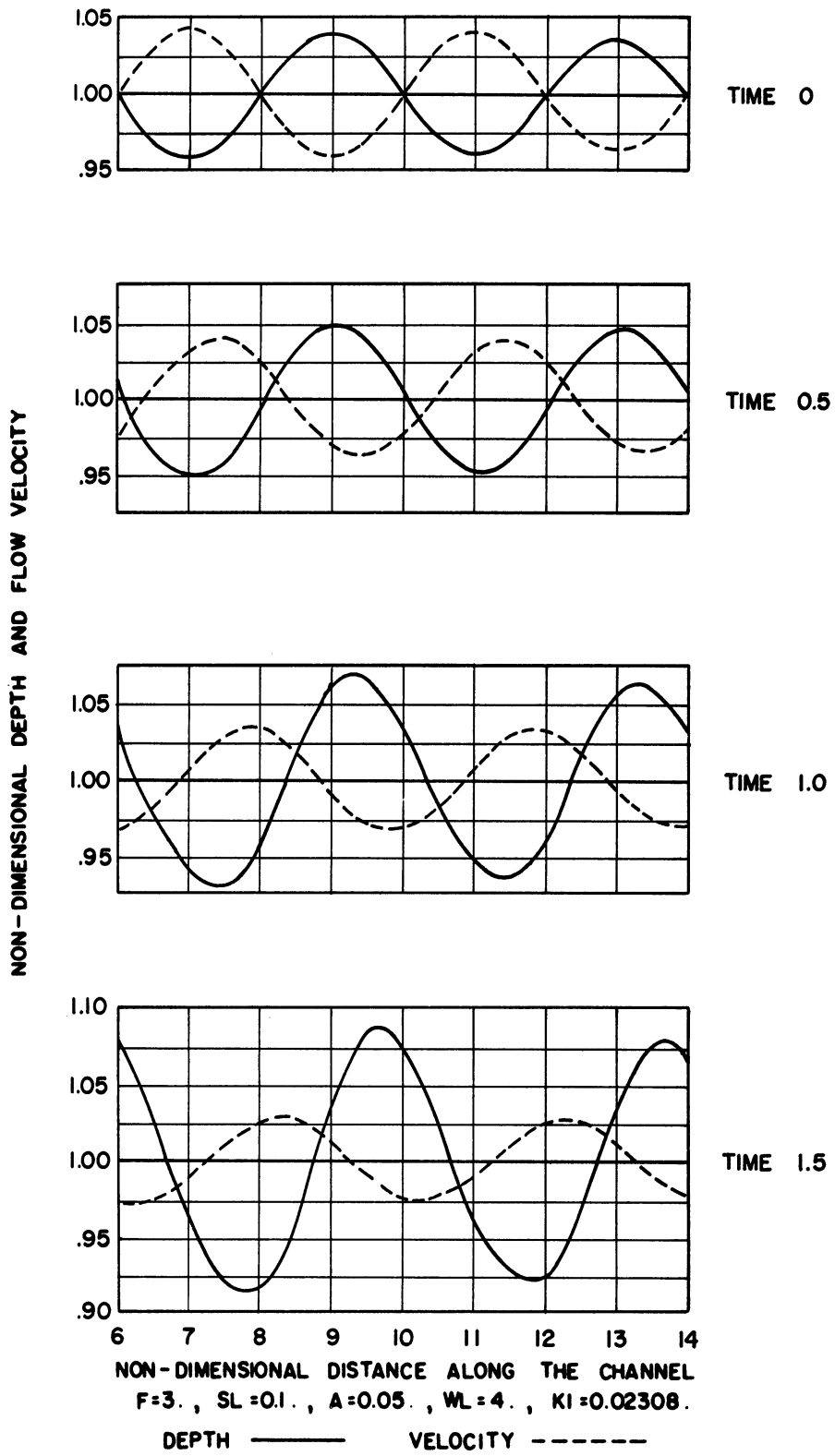


Figure 10a.

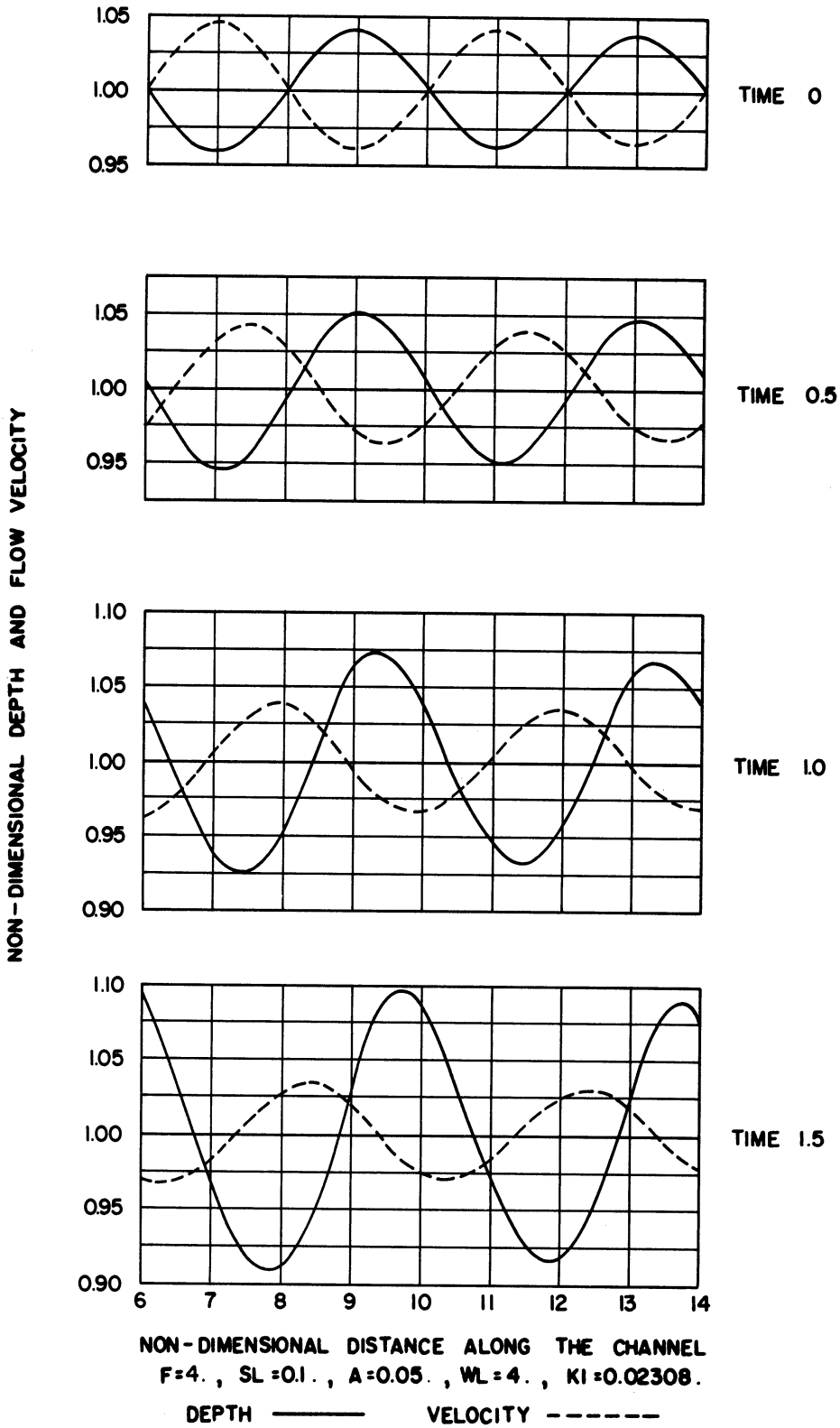


Figure 10b.

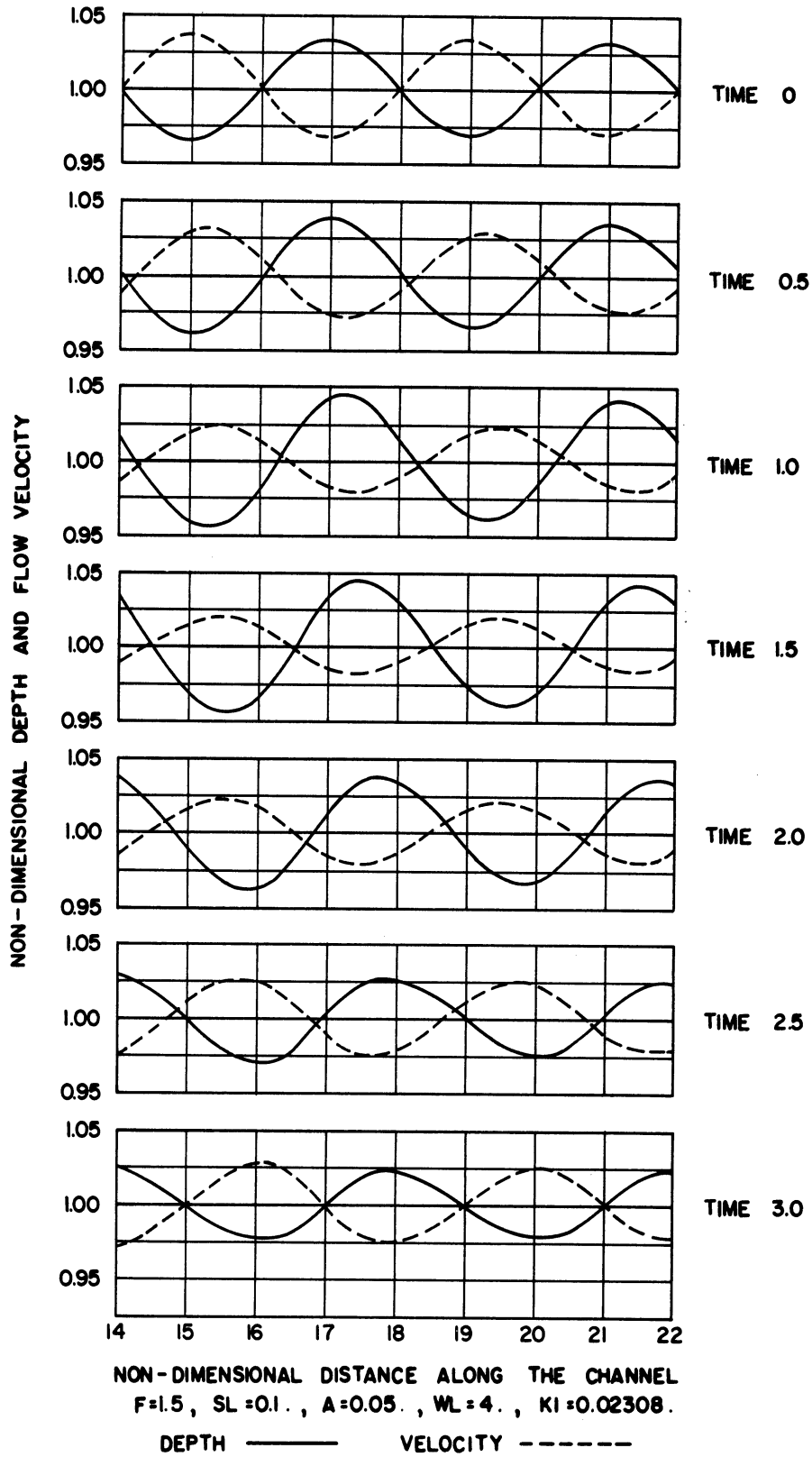


Figure 11a.

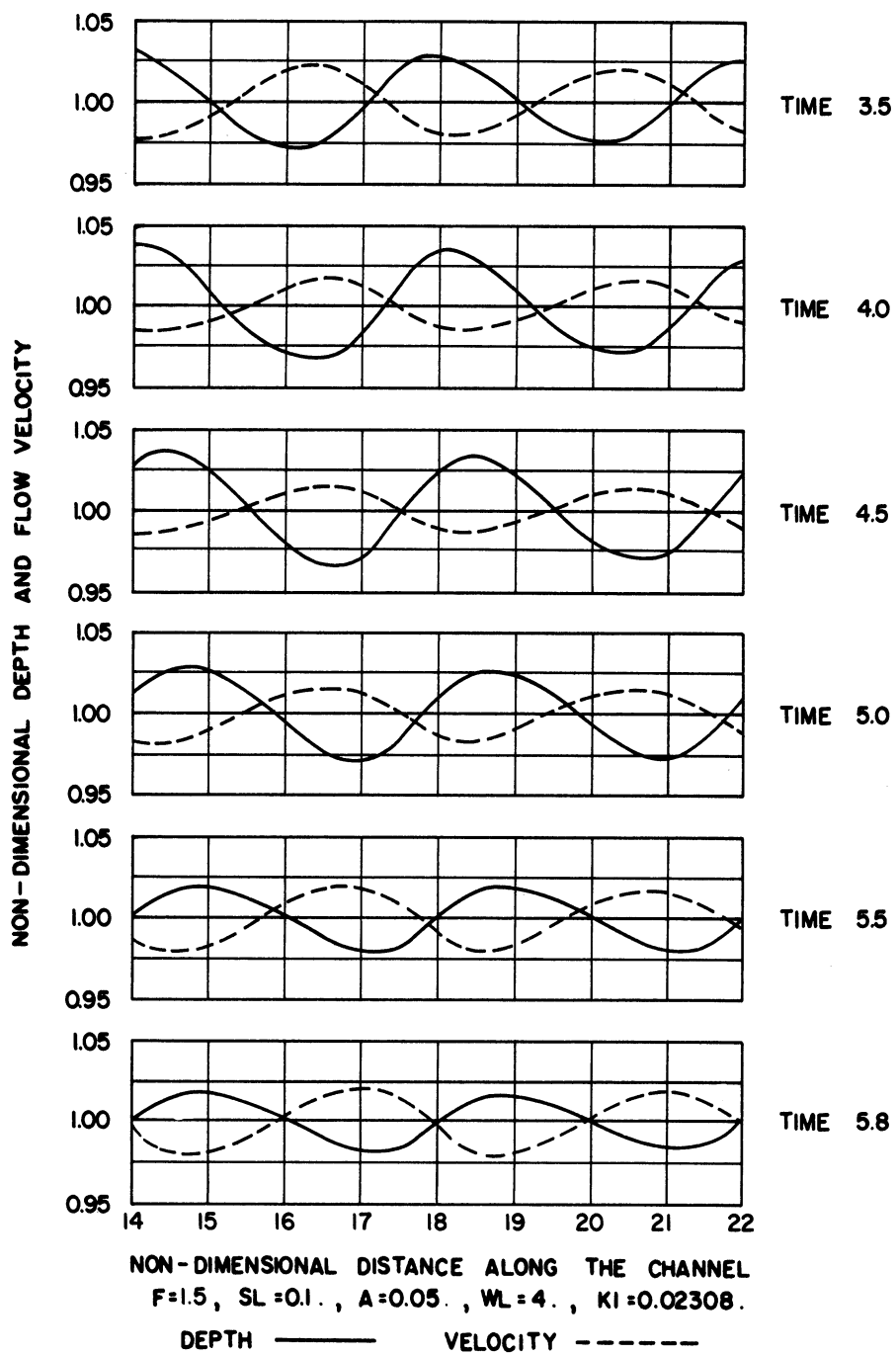


Figure 11b.

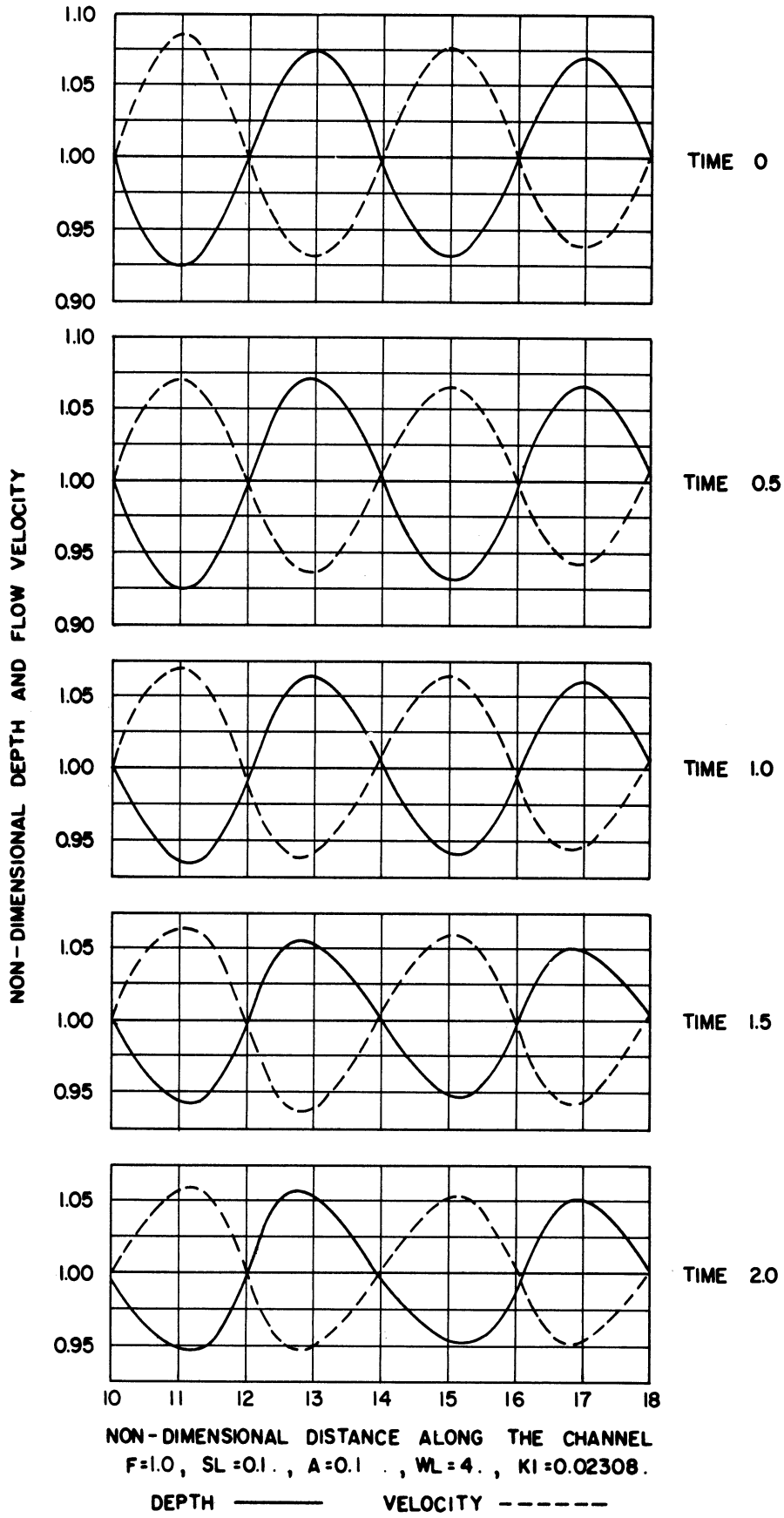


Figure 12a.

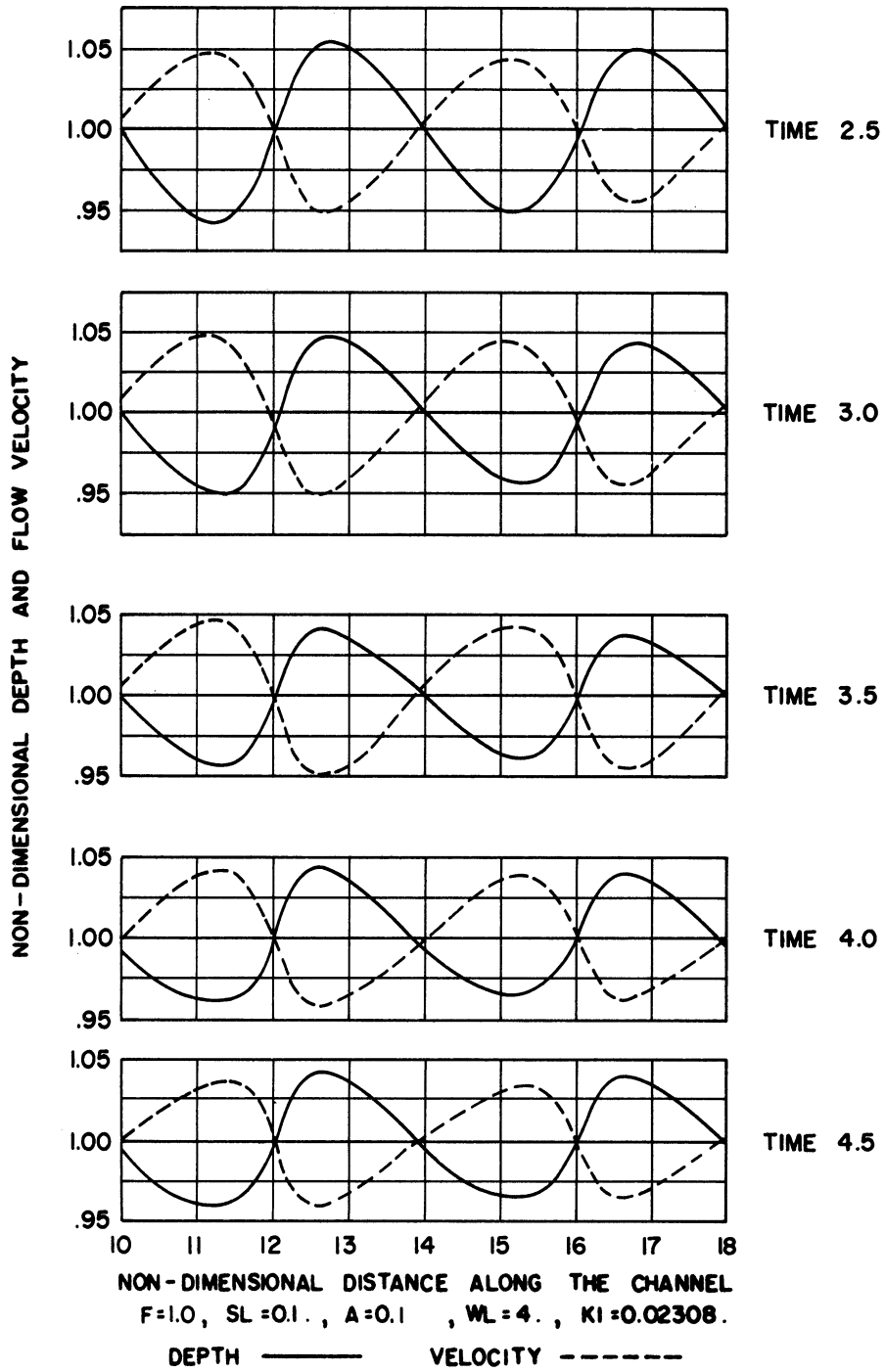


Figure 12b.

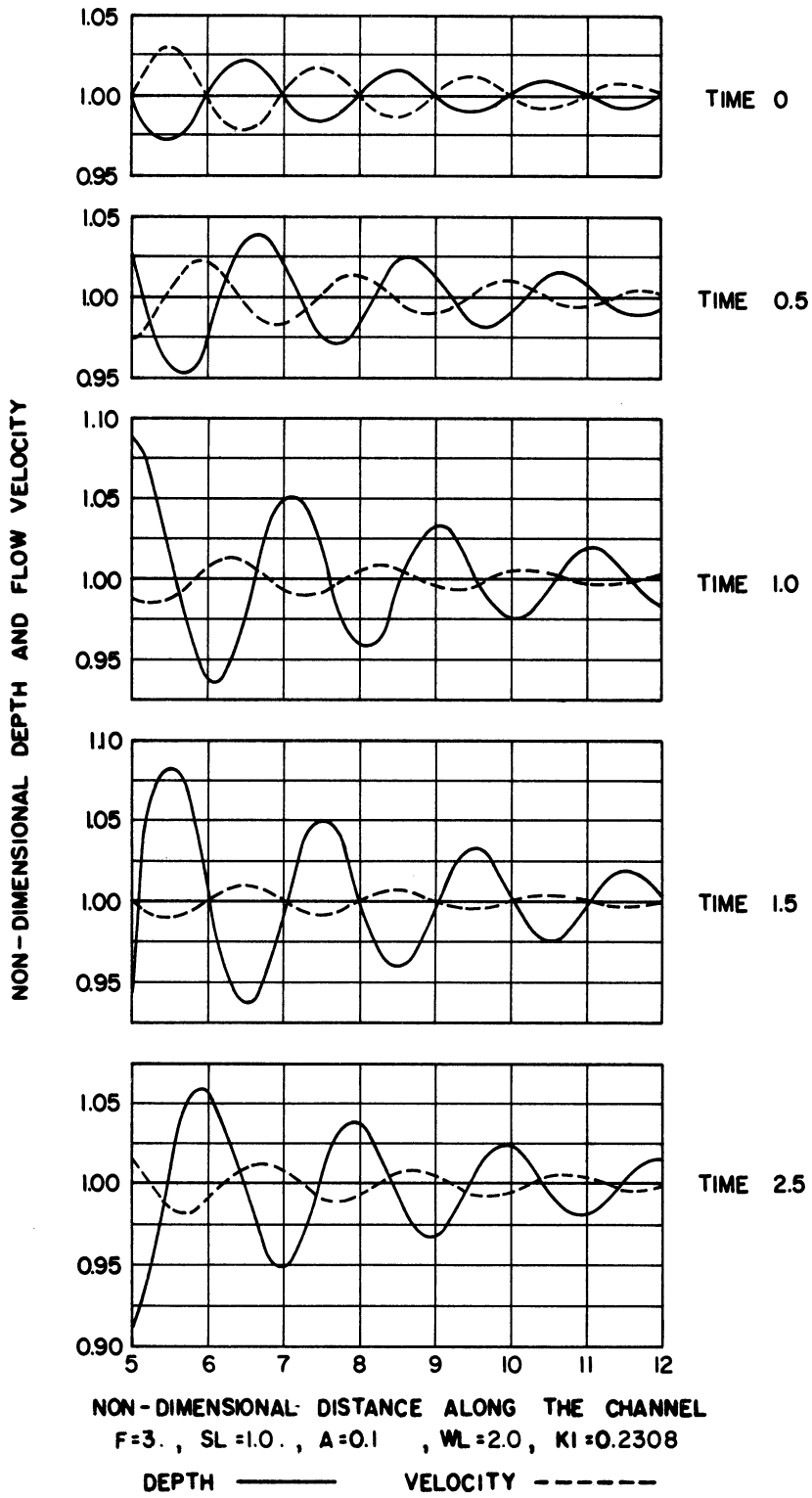


Figure 13.

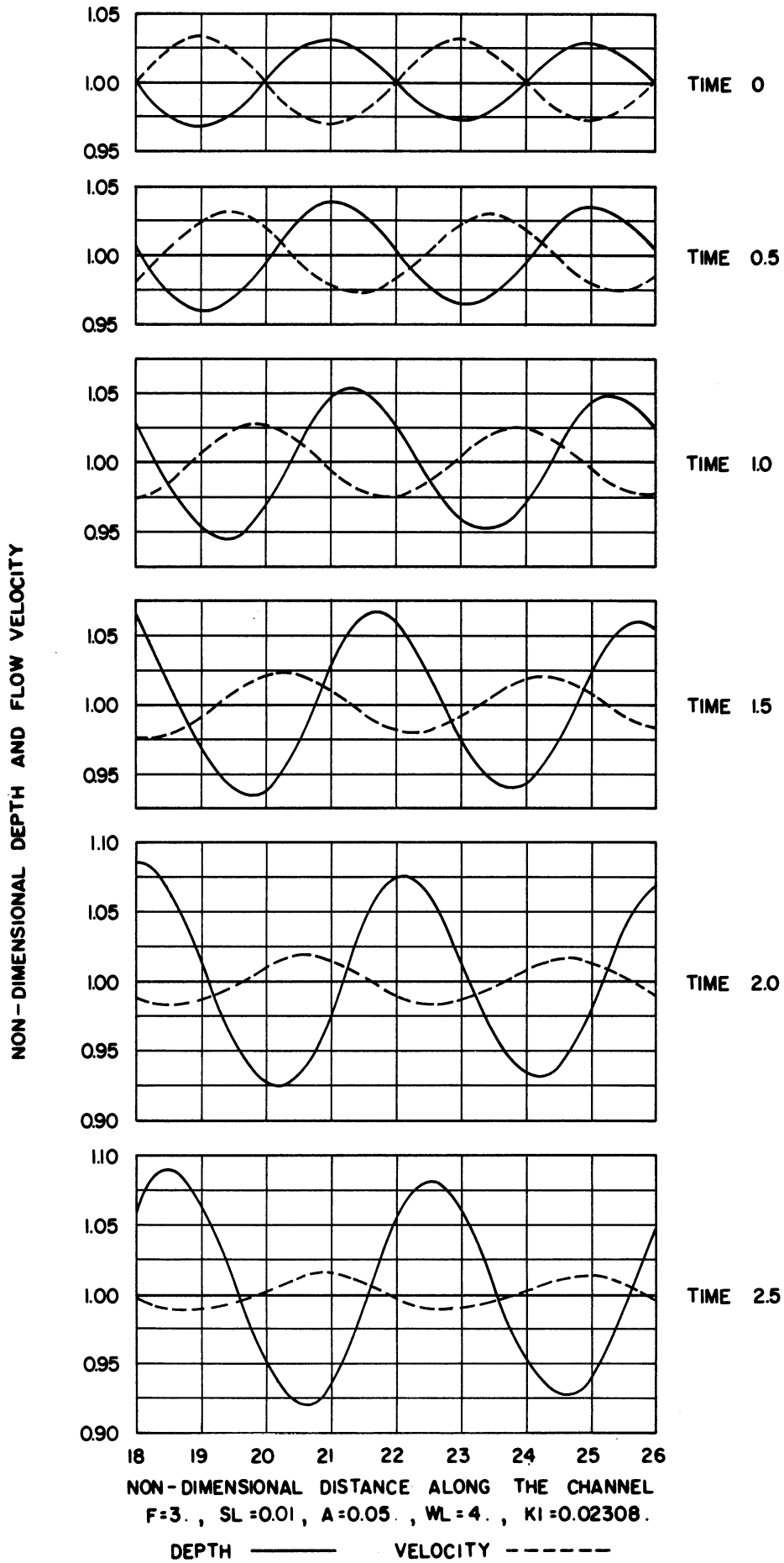


Figure 14a.

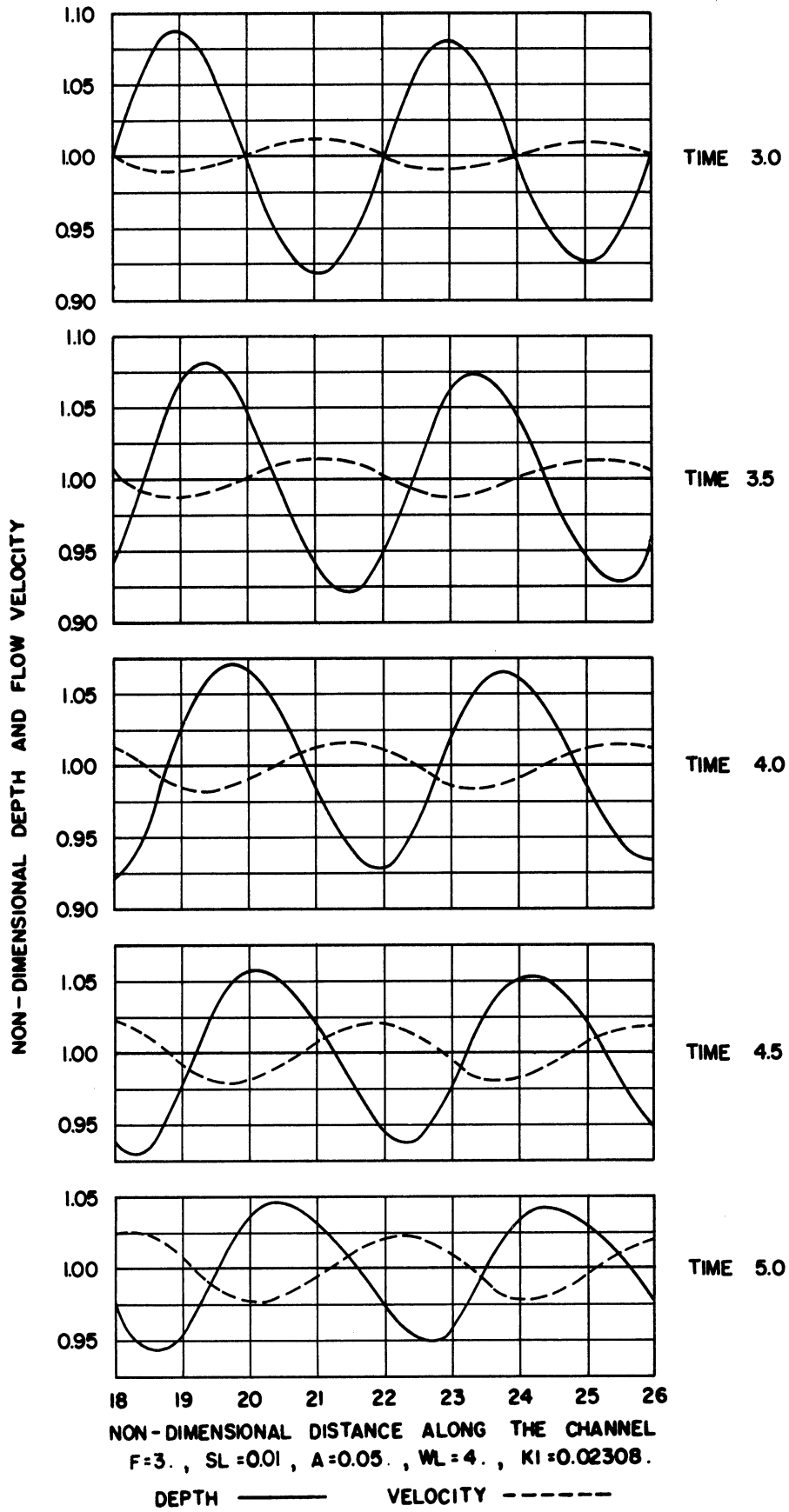


Figure 14b.

THE UNIVERSITY OF MICHIGAN
INDUSTRY PROGRAM OF THE COLLEGE OF ENGINEERING

THE DEVELOPMENT OF DISTURBANCES
IN SUPERCRITICAL FLOWS

James M. Wiggert

A dissertation submitted in partial fulfillment
of the requirements for the degree of
Doctor of Philosophy in the
University of Michigan
Department of Civil Engineering
1962

April, 1962

IP-558

Doctoral Committee:

Professor Ernest F. Brater, Co-Chairman
Professor Victor L. Streeter, Co-Chairman
Assistant Professor Walter R. Debler
Professor Maxwell O. Reade
Professor Chia-Shun Yih

12. Keulegan and Patterson. "A Criterion for Instability of Flow in Steep Channels." Trans. A.G.U., 21st Meeting, Part II, (1940) p. 594.
13. Mayer, P. "Roll Waves and Slug Flows in Inclined Open Channels." Trans. A.S.C.E., Vol. 126, Part I, (1961) p. 505.
14. Escoffier, F. F. "A Graphical Method for Investigating the Stability of Flow in Open Channels or in Closed Conduits Flowing Partly Full." Trans. A.G.U., Vol. 31, (1950) p. 583.
15. Yih, C-S. Stability of Parallel Laminar Flow With a Free Surface. Proc. 2nd U.S. Nat'l Congress of Appl. Mech. (Publ. by A.S.M.E.), (1954) p. 623.
16. Benjamin, T. B. "Wave Formation in Laminar Flow Down an Inclined Plane." J. Fluid Mech., Vol 2, (1957) p. 554. Corrections, Vol. 3, (1958) p. 657.
17. Craya, A. The Criterion for the Possibility of Roll Wave Formation. U.S. Nat'l. Bureau of Standards, Circ. No. 521, 1952.
18. Binnie, A. M. "Instability in a Slightly Inclined Water Channel." J. Fluid Mech., Vol. 5, (1949) p. 561.
19. Lister, M. "The Numerical Solutions of Partial Differential Equations by the Method of Characteristics." Mathematical Methods for Digital Computers. Ralston, A. and Wilf, H. S., editors. John Wiley and Sons, New York, 1960.
20. Cornish, Vaughn. Ocean Waves. Cambridge Univ. Press, 1934.
21. Lighthill, M. J. and Whitham, G. B. "On Kinematic Waves. I. Flood Movement in Long Rivers." Proc. Roy. Soc. of London, Vol. 229A, (May, 1955) p. 281.

APPENDIX

\$ COMPILE MAD, EXECUTE, DUMP, PRINT OBJECT, PUNCH OBJECT PRODD000

R NON-DIMENSIONAL CHARACTERISTIC SOLUTION.

R (FIRST ORDER ACCURACY)

R A PROGRAM TO EXAMINE THE EVOLUTION WITH TIME OF AN ARBITRARY

R WAVE SHAPE.

START READ DATA

R OUTPUT FORMAT FOR GENERAL HEADING.

PRINT COMMENT \$CHARACTERISTIC METHOD OF SOLUTION OF THE NON-
1DIMENSIONAL FLOW EQUATION\$S

PRINT COMMENT \$O $F*F*DU/DT+F*U*DU/DX+C*DC/DX*\cos(t$

1)- $\sin(t)+k*F*U/(C*C)=0$ \$

PRINT COMMENT \$O $C*DU/DX+2*U*DC/DX+2DC/DT=0$ \$

PRINT COMMENT \$OMULTIPLE DISTURBANCES ARE INTRODUCED FOR THE

1PURPOSE OF EXAMINING THE EVOLUTION OF WAVES WITH TIME.\$

PRINT COMMENTS THE DISTURBANCES EXTEND OVER THE ENTIRE INITIA

1L DATA. THE UPSTREAM TWO POINTS IN EACH COMPUTED ROW ARE\$

PRINT COMMENT \$ DROPPED IN THE SUCCEEDING ROW.\$

R BOOKKEEPING DECLARATIONS.

DIMENSION U1(1000), C1(1000), BIN(1000)

INTEGER I, J, K, L

L=1000

R INITIAL DATA OUTPUT.

PRINT FORMAT INFO, F, SL, XDEL, TDEL, A, TC, L, WL, KI

R DEFINITION STATEMENTS AND INITIALIZING.

SQC=SQRT.(1.-SL.P.2)

TSUM=0.

J=0

TH=TDEL/XDEL

EXECUTE AMP2.(UI, CI, XDEL, A, L, WL, KI)

R OUTPUT BLOCK FOR PRINTING RESULTS.

IOYA PRINT FORMAT T1, TSUM,J

PRINT COMMENT \$VELOCITIES

PRINT FORMAT T2, UI(J)..UI(1000)

PRINT COMMENT \$WAVE VELOCITIES

PRINT FORMAT T2, CI(J)..CI(1000)

PRINT COMMENT \$DEPTHSS

THROUGH ALPHA, FOR I=J, 1, I.G.1000

ALPHA BIN(I)=(CI(I)).P.2

PRINT FORMAT T2, BIN(J)..BIN(1000)

PRINT COMMENT \$X-DISTANCES

THROUGH BETA, FOR I=J, 1, I.G.1000-J

BETA BIN(I)=XDEL*(I+J)

PRINT FORMAT T3, BIN(J)..BIN(1000)

R PROGRESSIVE SUBSTITUTION STATEMENTS.

TSUM=TSUM+TDEL

UP1=U1(J)

CP1=C1(J)

UP=U1(J+1)

CP=C1(J+1)

R COMPUTATION BLOCK.

THROUGH ETA, FOR K=2+J, 1, K.G.1000

CHP=U1(K-1)+C1(K-1)*SQC/F

CHM=U1(K-1)-C1(K-1)*SQC/F

UR=U1(K)-TH*CHP*(U1(K)-U1(K-2))/2.

US=U1(K)-TH*CHM*(U1(K)-U1(K-1))

CR=C1(K)-TH*CHP*(C1(K)-C1(K-2))/2.

CS=C1(K)-TH*CHM*(C1(K)-C1(K-1))

U1(K-2)=UP1

C1(K-2)=CP1

UP1=UP

CP1=CP

UP=(UR+US)/2.+SQC*(CR-CS)/F+TDEL*SL*(1-(U1(K-1)/C1(K-1)).P.2
1)/F.P.2

ETA CP=(UR-US)*F/(4.+SQC)+(CR+CS)/2.

R FINAL SUBSTITUTION STATEMENTS.

U1(999)=UP1

C1(999)=CP1

U1(1000)=UP

C1(1000)=CP

2-13-62 4

R COMPUTATION INDEX INCREMENT.

J=J+2

R COMPLETION STOP AND LOCATION ASSIGNMENT.

WHENEVER TSUM.G.TC, TRANSFER TO OMEGA

TRANSFER TO IOTA

OMEGA PRINT COMMENT \$OPROGRAM COMPLETED\$

TRANSFER TO START

R FORMAY DECLARATIONS.

VECTOR VALUES T1=\$18H4WAVE FORM AT TIME F7.3, 21H, STARTING

1 INDEX IS 16*\$

VECTOR VALUES T2=\$120F6.3)*\$

VECTOR VALUES T3=\$120F6.1)*\$

VECTOR VALUES INFO=\$/24H PROUDE NUMBER =F10.3;/24H

1 SLOPE =F10.3;/24H DISTANCE INCREMENT =F10.3,

2/24H TIME INCREMENT =F10.3;/24H AMPLITUDE

3=F10.3;/24H GENERATION TIME =F10.3;/24H LIMIT ON STO

4RAGE =16;/24H INITIAL WAVE LENGTH=F10.3;/24H DECAY FA

5CTOR =F10.3*\$

END OF PROGRAM

\$ COMPILE MAD, PRINT OBJECT, PUNCH OBJECT

EXTF0000

R DUMMY ARGUMENT LIST AND FUNCTION LABEL.

EXTERNAL FUNCTION (U01, C01, X0, AA, LL, WWL, KK1)

ENTRY TO AMP2.

RNOTE THAT THIS EXTERNAL FUNCTION DEMANDS THAT WWL BE
R DIVISIBLE BY XD AN INTEGRAL NUMBER OF TIMES, AND THAT THE
R TOTAL NUMBER OF POINTS BE WITHIN THE STORAGE OF THE VECTOR

R =STORE=.

R FUNCTION BOOKKEEPING DECLARATIONS.

DIMENSION STORE(2000)

INTEGER I, LL

R FUNCTION IDENTIFICATION OUTPUT FORMAT.

PRINT COMMENT \$OTHE WAVE FORM IS AN EXPONENTIALLY DECAYING SI
INUSOIDAL WAVE, OF INDICATED WAVE LENGTH, AND DECAY FACTOR.\$

R INITIALIZING OF VARIABLE.

X=0.

R VARIABLE COMPUTATION BLOCK.

THROUGH F1, FOR I=0, 1, I.G.LL

STORE(I)=1.+AA*EXP.(-KK1*X)*SIN.(6.2831853*X/WWL)

UUI(I)=1./STORE(I)

CCI(I)=SQRT.(STORE(I))

F1 X=X+XD

FUNCTION RETURN

END OF FUNCTION

CHARACTERISTIC METHOD OF SOLUTION OF THE NON-DIMENSIONAL FLOW EQUATIONS

$F * F * DU / DT + F * F * U * DU / DX + C * DC / DX * COS(CT) - SIN(CT) + K * F * F * U * U / (C * C) = 0$

$C * DU / DX + 2 * U * DC / DX + 2 * DC / DT = 0$

MULTIPLE DISTURBANCES ARE INTRODUCED FOR THE PURPOSE OF EXAMINING THE EVOLUTION OF WAVES WITH TIME. THE DISTURBANCES EXTEND OVER THE ENTIRE INITIAL DATA. THE UPSTREAM TWO POINTS IN EACH COMPUTED ROW ARE DROPPED IN THE SUCCEEDING ROW.

FROUDE NUMBER = 3.000
SLOPE = .100
DISTANCE INCREMENT = .100
TIME INCREMENT = .100
AMPLITUDE = .100
GENERATION TIME = 7.000
LIMIT ON STORAGE = 1000
INITIAL WAVE LENGTH = 4.000
DECAY FACTOR = .023

THE WAVE FORM IS AN EXPONENTIALLY DECREAYING SINUSOIDAL WAVE, OF INDICATED WAVE LENGTH, AND DECAY FACTOR.

WAVE FORM AT TIME .000, STARTING INDEX IS 0

VELOCITIES

Table with 20 columns of velocity values. The first column is labeled 'VELOCITIES' and the rest contain numerical data points for each time step from 1.000 to 1.009.

1.000	.996	.992	.988	.984	.981	.979	.976	.975	.974	.974	.974	.975	.977	.979	.982	.985	.988	.992	.996
1.000	1.004	1.008	1.012	1.016	1.019	1.021	1.024	1.025	1.026	1.026	1.026	1.025	1.023	1.021	1.018	1.015	1.012	1.008	1.004
1.000	.996	.992	.989	.986	.983	.980	.979	.977	.976	.976	.976	.977	.979	.981	.983	.986	.989	.993	.996
1.000	1.004	1.007	1.011	1.014	1.017	1.019	1.021	1.023	1.024	1.024	1.024	1.023	1.021	1.019	1.017	1.014	1.011	1.007	1.004
1.000	.996	.993	.990	.987	.984	.982	.980	.979	.978	.978	.978	.979	.981	.982	.985	.987	.990	.993	.997
1.000	1.003	1.007	1.010	1.013	1.015	1.018	1.019	1.021	1.022	1.022	1.021	1.021	1.019	1.017	1.015	1.013	1.010	1.007	1.003
1.000	.997	.994	.991	.988	.986	.984	.982	.981	.980	.980	.980	.981	.982	.984	.986	.988	.991	.994	.997
1.000	1.003	1.006	1.009	1.012	1.014	1.016	1.018	1.019	1.020	1.020	1.020	1.019	1.017	1.016	1.014	1.011	1.009	1.006	1.003
1.000	.997	.994	.992	.989	.987	.985	.984	.983	.982	.982	.982	.983	.984	.985	.987	.989	.992	.994	.997
1.000	1.003	1.006	1.008	1.011	1.013	1.015	1.016	1.017	1.018	1.018	1.018	1.017	1.016	1.014	1.013	1.010	1.008	1.005	1.003
1.000	.997	.995	.992	.990	.988	.986	.985	.984	.984	.984	.984	.985	.987	.988	.990	.992	.995	.997	
1.000	1.003	1.005	1.008	1.010	1.012	1.013	1.015	1.016	1.016	1.016	1.016	1.016	1.014	1.013	1.011	1.009	1.007	1.005	1.002
1.000	.998	.995	.993	.991	.989	.988	.986	.985	.985	.985	.985	.986	.987	.988	.989	.991	.993	.995	.998
1.000	1.002	1.005	1.007	1.009	1.011	1.012	1.013	1.014	1.015	1.015	1.015	1.014	1.013	1.012	1.010	1.009	1.007	1.004	1.002
1.000	.998	.996	.994	.992	.990	.989	.988	.987	.986	.986	.986	.987	.988	.989	.990	.992	.994	.996	.998
1.000	1.002	1.004	1.006	1.008	1.010	1.011	1.012	1.013	1.013	1.014	1.013	1.013	1.012	1.011	1.009	1.008	1.006	1.004	1.002
1.000	.998	.996	.994	.992	.991	.990	.989	.988	.987	.987	.988	.988	.989	.990	.991	.993	.994	.996	.998
1.000	1.002	1.004	1.006	1.007	1.009	1.010	1.011	1.012	1.012	1.012	1.012	1.012	1.011	1.010	1.009	1.007	1.006	1.004	1.002
1.000	.998	.996	.995	.993	.992	.991	.990	.989	.989	.988	.989	.989	.990	.991	.992	.993	.995	.996	.998
1.000	1.002	1.004	1.005	1.007	1.008	1.009	1.010	1.011	1.011	1.011	1.011	1.011	1.010	1.009	1.008	1.007	1.005	1.003	1.002
1.000	.998	.997	.995	.994	.992	.991	.991	.990	.990	.989	.990	.990	.991	.992	.993	.994	.995	.997	.998
1.000	1.002	1.003	1.005	1.006	1.007	1.008	1.009	1.010	1.010	1.010	1.010	1.010	1.009	1.008	1.007	1.006	1.005	1.003	1.002

WAVE VELOCITIES

1.000	1.008	1.015	1.022	1.029	1.034	1.039	1.043	1.046	1.047	1.048	1.047	1.045	1.042	1.038	1.034	1.028	1.022	1.015	1.007
1.000	.993	.985	.978	.972	.966	.961	.957	.954	.953	.952	.953	.955	.958	.962	.967	.973	.979	.986	.993
1.000	1.007	1.014	1.020	1.026	1.031	1.036	1.039	1.042	1.043	1.044	1.043	1.041	1.039	1.035	1.031	1.026	1.020	1.013	1.007
1.000	.993	.987	.980	.974	.969	.965	.961	.958	.957	.957	.957	.959	.962	.965	.970	.975	.981	.987	.993
1.000	1.006	1.013	1.019	1.024	1.029	1.033	1.036	1.038	1.039	1.040	1.039	1.038	1.035	1.032	1.028	1.023	1.018	1.012	1.006
1.000	.994	.988	.982	.977	.972	.968	.965	.962	.961	.960	.961	.963	.965	.968	.973	.977	.983	.988	.994
1.000	1.006	1.012	1.017	1.022	1.026	1.030	1.033	1.035	1.036	1.036	1.036	1.034	1.032	1.029	1.026	1.021	1.016	1.011	1.006
1.000	.994	.989	.984	.979	.974	.971	.968	.966	.964	.964	.965	.966	.968	.971	.975	.979	.984	.989	.995
1.000	1.005	1.011	1.015	1.020	1.024	1.027	1.030	1.032	1.033	1.033	1.033	1.031	1.029	1.027	1.023	1.019	1.015	1.010	1.005
1.000	.995	.990	.985	.981	.977	.973	.971	.969	.968	.967	.968	.969	.971	.974	.977	.981	.985	.990	.995
1.000	1.005	1.010	1.014	1.018	1.022	1.025	1.027	1.029	1.030	1.030	1.030	1.029	1.027	1.024	1.021	1.018	1.014	1.009	1.005
1.000	.995	.991	.986	.982	.979	.976	.973	.971	.970	.970	.971	.972	.974	.976	.979	.983	.987	.991	.995
1.000	1.004	1.009	1.013	1.017	1.020	1.023	1.025	1.026	1.027	1.028	1.027	1.026	1.025	1.022	1.019	1.016	1.012	1.008	1.004
1.000	.996	.992	.988	.984	.981	.978	.976	.974	.973	.973	.973	.974	.976	.978	.981	.984	.988	.992	.996
1.000	1.004	1.008	1.012	1.015	1.018	1.021	1.023	1.024	1.025	1.025	1.025	1.024	1.022	1.020	1.018	1.015	1.011	1.008	1.004
1.000	.996	.992	.989	.985	.982	.980	.978	.976	.975	.975	.976	.977	.978	.980	.983	.986	.989	.993	.996
1.000	1.004	1.007	1.011	1.014	1.017	1.019	1.021	1.022	1.023	1.023	1.023	1.022	1.020	1.019	1.016	1.013	1.010	1.007	1.004
1.000	.996	.993	.990	.987	.984	.982	.980	.978	.978	.977	.978	.979	.980	.982	.984	.987	.990	.993	.997
1.000	1.003	1.007	1.010	1.013	1.015	1.017	1.019	1.020	1.021	1.021	1.021	1.020	1.019	1.017	1.015	1.012	1.009	1.006	1.003
1.000	.997	.994	.991	.988	.985	.983	.982	.980	.980	.979	.980	.981	.982	.984	.986	.988	.991	.994	.997
1.000	1.003	1.006	1.009	1.012	1.014	1.016	1.017	1.018	1.019	1.019	1.019	1.018	1.017	1.015	1.013	1.011	1.009	1.006	1.003
1.000	.997	.994	.991	.989	.987	.985	.983	.982	.981	.981	.982	.982	.983	.985	.987	.989	.992	.994	.997
1.000	1.003	1.006	1.008	1.010	1.013	1.014	1.016	1.017	1.017	1.018	1.017	1.017	1.016	1.014	1.012	1.010	1.008	1.005	1.003
1.000	.997	.995	.992	.990	.988	.986	.985	.984	.983	.983	.983	.984	.985	.986	.988	.990	.992	.995	.997
1.000	1.003	1.005	1.007	1.010	1.011	1.013	1.014	1.015	1.016	1.016	1.016	1.015	1.014	1.013	1.011	1.009	1.007	1.005	1.002
1.000	.998	.995	.993	.991	.989	.987	.986	.985	.985	.984	.985	.985	.986	.988	.989	.991	.993	.995	.998
1.000	1.002	1.005	1.007	1.009	1.010	1.012	1.013	1.014	1.014	1.015	1.014	1.014	1.013	1.012	1.010	1.008	1.007	1.004	1.002
1.000	.998	.996	.993	.992	.990	.988	.987	.986	.986	.986	.986	.987	.987	.989	.990	.992	.994	.996	.998
1.000	1.002	1.004	1.006	1.008	1.010	1.011	1.012	1.013	1.013	1.013	1.013	1.013	1.012	1.011	1.009	1.008	1.006	1.004	1.002
1.000	.998	.996	.994	.992	.991	.989	.988	.988	.987	.987	.987	.988	.989	.990	.991	.993	.994	.996	.998
1.000	1.002	1.004	1.006	1.007	1.009	1.010	1.011	1.012	1.012	1.012	1.012	1.011	1.010	1.009	1.007	1.005	1.004	1.002	
1.000	.998	.996	.995	.993	.992	.990	.989	.989	.988	.988	.988	.989	.990	.991	.992	.993	.995	.996	.998
1.000	1.002	1.004	1.005	1.007	1.008	1.009	1.010	1.011	1.011	1.011	1.011	1.011	1.010	1.009	1.008	1.006	1.005	1.003	1.002
1.000	.998	.997	.995	.994	.992	.991	.990	.990	.989	.989	.989	.990	.991	.991	.993	.994	.995	.997	.998
1.000	1.002	1.003	1.005	1.006	1.007	1.008	1.009	1.010	1.010	1.010	1.010	1.010	1.009	1.008	1.007	1.006	1.005	1.003	1.002

1.000	.998	.997	.996	.994	.993	.992	.991	.991	.990	.990	.990	.991	.991	.992	.993	.994	.996	.997	.999
1.000	1.001	1.003	1.004	1.006	1.007	1.008	1.008	1.009	1.009	1.009	1.009	1.009	1.008	1.007	1.006	1.005	1.004	1.003	1.001
1.000	.999	.997	.996	.995	.994	.993	.993	.992	.992	.992	.992	.992	.993	.994	.994	.995	.996	.998	.999
1.000	1.001	1.003	1.004	1.005	1.006	1.007	1.008	1.008	1.008	1.008	1.008	1.008	1.007	1.007	1.006	1.005	1.004	1.003	1.001
1.000	.999	.997	.996	.995	.994	.993	.993	.992	.992	.992	.992	.993	.994	.994	.995	.996	.997	.998	.999
1.000	1.001	1.002	1.004	1.005	1.006	1.007	1.007	1.007	1.007	1.007	1.007	1.007	1.006	1.006	1.005	1.004	1.003	1.002	1.001
1.000	.999	.998	.997	.996	.995	.994	.993	.993	.993	.993	.993	.994	.994	.995	.996	.997	.998	.999	.999
1.000	1.001	1.002	1.003	1.004	1.005	1.005	1.006	1.006	1.006	1.006	1.006	1.006	1.006	1.005	1.004	1.004	1.003	1.002	1.001
1.000	.999	.998	.997	.996	.996	.995	.994	.994	.994	.994	.994	.994	.995	.995	.996	.996	.997	.998	.999
1.000	1.001	1.002	1.003	1.003	1.004	1.005	1.005	1.006	1.006	1.006	1.006	1.006	1.005	1.005	1.004	1.003	1.003	1.002	1.001
1.000	.999	.998	.997	.996	.996	.995	.995	.995	.995	.994	.994	.994	.995	.995	.996	.996	.997	.998	.999
1.000	1.001	1.002	1.002	1.003	1.004	1.004	1.005	1.005	1.005	1.005	1.005	1.005	1.005	1.004	1.004	1.003	1.002	1.002	1.001
1.000	.999	.998	.998	.997	.996	.996	.995	.995	.995	.995	.995	.995	.995	.996	.996	.997	.998	.998	.999
1.000																			

DEPTHS

1.000	1.016	1.031	1.045	1.058	1.070	1.080	1.088	1.093	1.097	1.098	1.096	1.093	1.086	1.078	1.068	1.057	1.044	1.030	1.015
1.000	.985	.971	.957	.944	.933	.924	.916	.911	.908	.907	.908	.912	.917	.925	.935	.946	.958	.972	.986
1.000	1.014	1.028	1.041	1.053	1.064	1.073	1.080	1.085	1.088	1.089	1.088	1.084	1.079	1.071	1.062	1.052	1.040	1.027	1.014
1.000	.986	.973	.961	.949	.939	.931	.924	.919	.916	.915	.916	.919	.925	.932	.941	.951	.962	.974	.987
1.000	1.013	1.026	1.037	1.048	1.058	1.066	1.073	1.078	1.080	1.081	1.080	1.077	1.072	1.065	1.057	1.047	1.036	1.025	1.012
1.000	.988	.976	.964	.954	.945	.937	.930	.926	.923	.922	.924	.927	.931	.938	.946	.955	.965	.976	.988
1.000	1.012	1.023	1.034	1.044	1.053	1.060	1.066	1.071	1.073	1.074	1.073	1.070	1.066	1.059	1.052	1.043	1.033	1.022	1.011
1.000	.989	.978	.967	.958	.949	.942	.937	.932	.930	.929	.930	.933	.937	.943	.951	.959	.968	.979	.989
1.000	1.011	1.021	1.031	1.040	1.048	1.055	1.061	1.065	1.067	1.068	1.067	1.064	1.060	1.054	1.047	1.039	1.030	1.020	1.010
1.000	.990	.980	.970	.962	.954	.947	.942	.938	.936	.936	.936	.939	.943	.948	.955	.963	.971	.980	.990
1.000	1.010	1.019	1.028	1.037	1.044	1.050	1.055	1.059	1.061	1.062	1.061	1.058	1.054	1.049	1.043	1.036	1.028	1.019	1.009
1.000	.991	.981	.973	.965	.958	.952	.947	.944	.942	.941	.942	.944	.948	.953	.959	.966	.974	.982	.991
1.000	1.009	1.018	1.026	1.033	1.040	1.046	1.050	1.054	1.056	1.056	1.055	1.053	1.050	1.045	1.039	1.033	1.025	1.017	1.009
1.000	.991	.983	.975	.968	.962	.956	.952	.949	.947	.946	.947	.949	.953	.957	.963	.969	.976	.984	.992
1.000	1.008	1.016	1.024	1.031	1.037	1.042	1.046	1.049	1.051	1.051	1.050	1.048	1.045	1.041	1.036	1.030	1.023	1.016	1.008
1.000	.992	.985	.977	.971	.965	.960	.956	.953	.952	.951	.952	.954	.957	.961	.966	.972	.978	.985	.993
1.000	1.007	1.015	1.022	1.028	1.033	1.038	1.042	1.045	1.046	1.047	1.046	1.044	1.041	1.037	1.033	1.027	1.021	1.014	1.007
1.000	.993	.986	.979	.973	.968	.964	.960	.957	.956	.955	.956	.958	.961	.964	.969	.974	.980	.986	.993
1.000	1.007	1.013	1.020	1.025	1.030	1.035	1.038	1.041	1.042	1.043	1.042	1.040	1.038	1.034	1.030	1.025	1.019	1.013	1.007
1.000	.994	.987	.981	.976	.971	.967	.964	.961	.960	.959	.960	.962	.964	.967	.972	.976	.982	.988	.994
1.000	1.006	1.012	1.019	1.023	1.028	1.032	1.035	1.037	1.038	1.039	1.038	1.037	1.034	1.031	1.027	1.023	1.017	1.012	1.006
1.000	.994	.988	.983	.978	.973	.970	.967	.965	.963	.963	.963	.965	.967	.970	.974	.979	.983	.989	.994
1.000	1.006	1.011	1.016	1.021	1.025	1.029	1.032	1.034	1.035	1.035	1.035	1.034	1.031	1.028	1.025	1.021	1.016	1.011	1.005
1.000	.995	.989	.984	.980	.976	.972	.970	.968	.967	.966	.967	.968	.970	.973	.976	.980	.985	.990	.995
1.000	1.005	1.010	1.015	1.019	1.023	1.026	1.029	1.031	1.032	1.032	1.032	1.031	1.029	1.026	1.023	1.019	1.014	1.010	1.005
1.000	.995	.990	.986	.982	.978	.975	.972	.971	.969	.969	.970	.971	.973	.975	.978	.982	.986	.991	.995
1.000	1.005	1.009	1.014	1.018	1.021	1.024	1.026	1.028	1.029	1.029	1.029	1.028	1.026	1.024	1.021	1.017	1.013	1.009	1.005
1.000	.996	.991	.987	.983	.980	.977	.975	.973	.972	.972	.972	.973	.975	.977	.980	.984	.987	.991	.996
1.000	1.004	1.008	1.012	1.016	1.019	1.022	1.024	1.026	1.027	1.027	1.026	1.025	1.024	1.022	1.019	1.016	1.012	1.008	1.004
1.000	.996	.992	.988	.985	.982	.979	.977	.976	.975	.974	.975	.976	.977	.979	.982	.985	.989	.992	.996
1.000	1.004	1.008	1.011	1.015	1.017	1.020	1.022	1.023	1.024	1.024	1.024	1.023	1.022	1.020	1.017	1.014	1.011	1.007	1.004
1.000	.996	.993	.989	.986	.983	.981	.979	.978	.977	.977	.977	.978	.979	.981	.984	.986	.990	.993	.996
1.000	1.004	1.007	1.010	1.013	1.016	1.018	1.020	1.021	1.022	1.022	1.022	1.021	1.020	1.018	1.016	1.013	1.010	1.007	1.003
1.000	.997	.993	.990	.987	.985	.983	.981	.980	.979	.979	.979	.980	.981	.983	.985	.988	.990	.994	.997
1.000	1.003	1.006	1.009	1.012	1.015	1.017	1.018	1.019	1.020	1.020	1.020	1.019	1.018	1.016	1.014	1.012	1.009	1.006	1.003
1.000	.997	.994	.991	.988	.986	.984	.983	.981	.981	.981	.981	.982	.983	.984	.986	.989	.991	.994	.997
1.000	1.003	1.006	1.009	1.011	1.013	1.015	1.017	1.018	1.018	1.018	1.018	1.018	1.018	1.016	1.015	1.013	1.011	1.008	1.006
1.000	.997	.994	.992	.989	.987	.986	.984	.983	.982	.982	.983	.983	.984	.986	.988	.990	.992	.995	.997
1.000	1.003	1.005	1.008	1.010	1.012	1.014	1.015	1.016	1.017	1.017	1.017	1.016	1.015	1.014	1.012	1.010	1.008	1.005	1.003
1.000	.997	.995	.993	.990	.988	.987	.986	.985	.984	.984	.984	.985	.986	.987	.989	.991	.993	.995	.998
1.000	1.002	1.005	1.007	1.009	1.011	1.013	1.014	1.015	1.015	1.015	1.015	1.015	1.015	1.014	1.012	1.011	1.009	1.007	1.005
1.000	.998	.995	.993	.991	.989	.988	.987	.986	.985	.985	.985	.986	.987	.988	.990	.991	.993	.996	.998

